Florida thunderstorms: A faucet of reactive nitrogen to the upper troposphere

B. Ridley,[1] L. Ott,[2] K. Pickering,[2] L. Emmons,[1] D. Montzka,[1] A. Weinheimer,[1] D. Knapp,[1] F. Grahek,[1] L. Li,[3] G. Heymsfield,[4] M. McGill,[4] P. Kucera,[5] M. J. Mahoney,[6] D. Baumgardner,[7] M. Schultz,[8] and G. Brasseur[8]

Received 12 March 2004; revised 15 June 2004; accepted 12 July 2004; published 8 September 2004.

[1] During the July 2002 Cirrus Regional Study of Tropical Anvils and Cirrus Layers-Florida Area Cirrus Experiment (CRYSTAL-FACE), flights of a WB-57F aircraft revealed mixing ratios of nitric oxide 10–50 times background over distances of 25–175 km in the anvils of thunderstorms and in clear air downwind of storm systems due to lightning activity and possible transport from the boundary layer. Estimates of the total mass of NO_x injected into the middle and upper troposphere differed considerably for a moderately versus highly electrically active storm system as expected. However, assuming that the total mass is dominated by lightning production, rough estimates of the production per average lightning flash for a moderately and a highly active storm also yielded quite different ranges of $(0.33–0.66) \times 10^{26}$ and $(1.7–2.3) \times 10^{26}$ molecules NO/flash, respectively. If the common assumption is made that intracloud flashes have 1/10th the NO production efficiency of cloud-to-ground (CG) flashes, the ranges of production for the moderately and highly active storms were $(0.88–1.8) \times 10^{26}$ and $(4.5–6.1) \times 10^{26}$ molecules NO/CG flash, respectively. The observed CG flash accumulations and NO_x mass production estimate for the month of July 2002 over the Florida area are compared with results from the MOZART-2 global chemistry-transport model that uses a common lightning flash parameterization. Reasonable agreement was found after a correction to the lightning parameterization was made. Finally, broad-scale median mixing ratios of NO within anvils over Florida were significantly larger than found in storms previously investigated over Colorado and New Mexico. *INDEX TERMS:* 0322 Atmospheric Composition and Structure: Constituent sources and sinks; 0320 Atmospheric Composition and Structure: Cloud physics and chemistry; 0365 Atmospheric Composition and Structure: Troposphere—composition and chemistry; 0368 Atmospheric Composition and Structure: Troposphere—constituent transport and chemistry; *KEYWORDS:* NO_x, nitric oxide, lightning, convection, thunderstorms

Citation: Ridley, B., et al. (2004), Florida thunderstorms: A faucet of reactive nitrogen to the upper troposphere, *J. Geophys. Res.*, *109*, D17305, doi:10.1029/2004JD004769.

1. Introduction

[2] The global production of nitric oxide by lightning discharges remains uncertain with a range of perhaps 2–20 Tg(N)/yr [*World Meteorological Organization* (*WMO*), 1995]. In comparison, current global emissions of reactive nitrogen (NO_x = NO + NO_2) from combustion and soil sources are ~46 Tg(N)/yr [*Intergovernmental Panel on Climate Change* (*IPCC*), 2001]. More recent estimates of NO production by lightning, determined from a re-evaluation of earlier work or from first principles, give 12–13 Tg(N)/yr [*Price et al.*, 1997a, 1997b]. *Nesbitt et al.* [2000] have estimated 0.9–9 Tg(N)/yr based upon analysis of global lightning flash frequencies from the optical transient detector (OTD) satellite instrument, the range reflecting uncertainty in estimates of the production of NO per flash. *Huntrieser et al.* [1998] have summarized a wide range of estimates of 0.7–220 Tg(N)/yr from a review of field studies of individual storms. Given the complexity of deep convective processes alone, combined with the uncertainties in the physics of individual lightning flashes, the concept of an average production of NO per lightning flash or average yearly production must include a large possible variance.

[1] Atmospheric Chemistry Division, National Center for Atmospheric Research, Boulder, Colorado, USA.
[2] Department of Meteorology, University of Maryland, College Park, Maryland, USA.
[3] Goddard Earth Sciences and Technology Center, University of Maryland, Baltimore, Maryland, USA.
[4] Mesoscale Atmospheric Processes Branch, NASA Goddard Space Flight Center, Greenbelt, Maryland, USA.
[5] Department of Atmospheric Sciences, University of North Dakota, Grand Forks, North Dakota, USA.
[6] Jet Propulsion Laboratory, California Institute of Technology, Pasadena, California, USA.
[7] Centro de Ciencias de la Atmosfera, Universidad Nacional Autonoma de Mexico, Mexico D. F., Mexico.
[8] Max Planck Institute für Meteorologie, Hamburg, Germany.

0148-0227/04/2004JD004769$09.00

[3] Most global chemistry-transport models (CTMs) use total amounts of 3–7 Tg(N)/yr from lightning production based on deriving general agreement between the particular model's prediction of the NO_x distribution and available airborne and other measurements. CTMs have also been used in an inverse sense to examine the likely range of global lightning production [*Levy et al.*, 1996; *Lamarque et al.*, 1996; *Flatøy and Hov*, 1997]. In practice, the lightning source term in CTMs is currently subgrid-scale and the total amount used in individual models has changed as improvements in convective parameterizations, stratosphere-troposphere coupling, or updates to other emission inventories have been implemented. A summary of lightning source strengths and changes made in a number of CTMs is presented in Table 1 of *Zhang et al.* [2003a].

[4] Advances have been made using satellite-borne sensors to provide more accurate climatology for lightning flash rates and their geographic and temporal distributions. The global average flash rate (cloud-to-ground (CG) plus intracloud (IC) flashes) has recently been reduced from the much earlier and widely used estimate of 100 s^{-1} [*Brooks*, 1925] to 44 ± 5 s^{-1} [*Christian et al.*, 2003]. This reduction by 0.44 would have a nearly proportional impact on many of the earlier estimates of global production reviewed by *Lawrence et al.* [1995] and *Huntrieser et al.* [1998]. In combination with ground-based networks that primarily detect CG flashes, the satellite data have also provided refined climatology of the IC/CG ratio for specific continental regions [*Boccippio et al.*, 2001]. This ratio is important because the more frequent IC flashes are generally assumed to be an order of magnitude less efficient than CG flashes in producing NO. However, modeling and observational evidence now suggests that the production per IC flash is ~1/2 or more of the production per CG flash for some thunderstorms [*Gallardo and Cooray*, 1996; *DeCaria et al.*, 2000; *Dye et al.*, 2000; *Huntrieser et al.*, 2002; *Skamarock et al.*, 2003; *Zhang et al.*, 2003a; *Fehr et al.*, 2004]. Recently, *Théry et al.* [2000] derived a production of 3.0×10^{26} molecules of NO (6.9 kg(N), range 0.14–9.6 kg(N)) per IC flash from measurements with a lightning interferometer. This value is significantly larger than the 0.67×10^{26} molecules of NO/IC flash (1.5 kg(N)/IC flash) recommended by *Price et al.* [1997a], the value that is used in many models of continental storms. If IC and CG flashes were comparable in average production and as large as 6.7×10^{26} molecules/flash, then the global flash rate of 44 s^{-1} would yield a global production of 22 Tg(N)/yr or 3–7 times the source strength used in most CTMs. It seems quite unlikely that the large ensemble of different CTM models currently in use underestimate the lightning source by such a large factor. Thus either the production per IC flash is comparable to that per CG flash for only a small fraction of the number of storms that occur globally or the average production per CG flash recommended by Price et al. is too large.

[5] Although satellite sensors have provided a much better climatology of lightning flashes another issue has emerged with the use of ground-based lightning interferometers that have the ability to accurately locate IC and CG lightning discharges. Their sensitivity allows detection of many more discharges than would be recorded by conventional IC or total flash measurement techniques or current satellite sensors [*Dye et al.*, 2000; *Théry et al.*, 2000; *Defer et al.*, 2001; *Skamarock et al.*, 2003]. It is not clear whether the very short lived or weaker discharges recorded by the interferometers are significant sources of reactive nitrogen.

[6] From the perspective of tropospheric ozone production or HO_x ($OH + HO_2$) radical budgets, the altitude distribution of NO_x generated by thunderstorms is as important as knowledge of the total production [*Ridley et al.*, 1996]. For example, *Tie et al.* [2002] showed that their CTM gave equally good agreement with airborne observations of NO_x in the middle and upper troposphere (UT) using a global source of 7 Tg(N)/yr in which the production per storm was distributed uniformly by mass over all altitudes of the model storms or by using a source of one-half as much distributed over only the upper region of the storms. (Equal mass at each model level of course yields increasing mixing ratios with increasing altitude.) Previous thunderstorm studies have measured large increases of NO_x in the anvil outflow or above about 7 km as would be expected from storm dynamics [*Dickerson et al.*, 1987; *Ridley et al.*, 1996; *Huntrieser et al.*, 1998, 2002; *Stith et al.*, 1999; *Dye et al.*, 2000]. The anvil, which expands (or is stretched depending on local winds) with increasing input from below, acts as an accumulator of lightning-produced NO (IC + CG) that is generated within the anvil region or within or near the updraft regions of the convective core(s). (Anvil outflows are often fed by more than one convective cell.) The anvil also accumulates possible input of "pollutant" NO_x (and other chemical constituents including water) from the lower troposphere and boundary layer (LT/BL) that feeds the convective core(s). "Pollutant" input will of course depend strongly on the proximity of the storm to surface sources and this input can change as the storm propagates over the surface. Clearly, the impact of electrically active deep convection on the NO_x budget in the UT, and the consequent impact on the ozone budget, is not only limited to NO_x production by lightning.

[7] The altitude distribution of NO_x resulting from electrically active deep convection is important because the lifetime of NO_x in the UT is usually much longer than in the lower troposphere, several days to a week versus a few hours in the polluted boundary layer [*Ehhalt et al.*, 1992]. The lifetime will also depend on the transport of other reactive constituents including water in the convective event. Thus NO_x from lightning or that transported from the LT/BL through the storm into the UT can have chemical consequences over areas much broader than the scale of a typical active storm. There are many examples of observations of large NO_x plumes in the UT that have been attributed to the occurrence of lightning activity in deep convection that occurred 2–3 days upwind of the observations [*Pickering et al.*, 1996; *Jeker et al.*, 2000; *Crawford et al.*, 2000; *Brunner et al.*, 2001; *Lange et al.*, 2001].

[8] Observations from aircraft studies have had a strong impact on recommendations for improved model parameterizations in which a much larger fraction of the reactive nitrogen mass is deposited into the UT [*Ridley et al.*, 1996; *Pickering et al.*, 1998; *Allen and Pickering*, 2002]. However, the aircraft studies have not been able to determine quantitatively the fraction of accumulated lightning production that results in net injection of NO_x to the UT, say above

6–7 km, versus that to the lower troposphere. It is likely to be highly variable and at least depend upon the IC/CG ratio. Storms can also have a significant fraction of CG flash lengths external to the core region where there is little chance of subsequent vertical transport into the anvil. Downdrafts may also distribute lightning-produced NO to low altitudes. Detailed 2-D and 3-D simulations with cloud resolving models have provided some insight, but most of these models do not contain ab initio lightning generation so the conclusions are sensitive to assumptions made about the placement of especially CG- and to a lesser extent IC-produced NO within the storm. Nevertheless, these models suggest that 55–85% of the total mass of reactive nitrogen produced by lightning is deposited above 6–7 km [*Pickering et al.*, 1998; *Skamarock et al.*, 2003]. As expected, the fraction approaches 100% for storms dominated strongly by IC activity [*DeCaria et al.*, 2000; *Skamarock et al.*, 2003; *Fehr et al.*, 2004]. These models also predict that significant input to the storm core(s) is not from the lowest part of the boundary layer but is dominated by input from nearer its top and the lower "free" troposphere, a result that may be sensitive to how the model storm convection is initiated. More recently, *Zhang et al.* [2003a, 2003b] have reported on storm models that for the first time employ explicit lightning physics.

[9] The integrated chemical impact of the storm after maturity and subsequent mixing/dilution requires detailed modeling because the chemistry is nonlinear [e.g., *Pickering et al.*, 1992, 1996; *Crawford et al.*, 2000; *Meijer et al.*, 2000; *Zhang et al.*, 2003]. Injections of NO_x of the order of 1 ppbv will significantly increase the local net rate of ozone production in the UT, while injections of more than a few ppbv can saturate and even decrease the net production rate. The actual saturation mixing ratio will depend sensitively on the production of and partitioning of HO_x radicals including organic peroxy radicals [*Ehhalt and Rohrer*, 1995]. With the longer lifetime, and because daytime partitioning of NO_x strongly favors NO in the near-cloud free UT, NO is a good tracer of lightning production and the possible downwind impact. At 12.5 km altitude with ozone at 80–100 ppbv and noontime clear skies at 26°N in July, the steady state ratio of $NO_x/NO \sim (1+ k[O_3]/J_{NO2})^{-1}$ is 1.14–1.17 where J_{NO2} is the local photolysis rate of NO_2 and k is the rate coefficient for oxidation of NO to NO_2 by O_3. Enhanced actinic flux that occurs above or within the upper regions of anvil clouds can increase the clear sky J_{NO2} by a factor of ~2 and therefore further decrease the NO_x/NO ratio [*Madronich*, 1987].

[10] In June through mid-August, convergent low-altitude flows over the Florida peninsula generate extensive thunderstorm activity during the day and night. Over the month of July 2002 the southern half of the Florida peninsula experienced more than a quarter million CG flashes and, from climatology [*Boccippio et al.*, 2001], likely more than an additional half million IC flashes. During this month, measurements of NO and other constituents were made from a WB-57F high-altitude aircraft about and within the anvils of some of these thunderstorms as one component of the NASA Cirrus Regional Study of Tropical Anvils and Cirrus Layers-Florida Area Cirrus Experiment (CRYSTAL-FACE) (http://cloud1.arc.nasa.gov/crystalface/). Here we discuss observations of NO produced by some Florida thunderstorms and compare the mixing ratios with those from thunderstorms over other regions of the United States and with results from one version of a CTM, the Model for Ozone and Related Tracers (MOZART-2) [*Brasseur et al.*, 1998a; *Horowitz et al.*, 2003].

2. Experiment

[11] The NASA WB-57F and 5 other aircraft that participated in CRYSTAL-FACE were based at the Boca Chica Naval Air Station located near Key West, Florida (24.6°N, 81.7°W). A total of 14 flights were made with the WB-57F including the transit flights from or to Houston, Texas on June 29 and July 31, 2002. Nine of the flights had portions that probed the anvils of storms above ~10 km altitude and all flights had excursions into the lower stratosphere, sometimes to as high as ~19 km altitude. (Altitudes given here are geometric altitudes above mean sea level determined by the Global Positioning System (GPS) instrument on the aircraft.)

[12] NO was measured using a four-channel chemiluminescence instrument [*Ridley et al.*, 2004] located in the rear pallet of the aircraft. Ambient air was sampled through an inlet contained in an airfoil and at a distance of 21 cm from the bottom of the pallet, which forms the lower fuselage of the aircraft. Mixing ratios presented are for 1-s intervals corresponding to horizontal distances of 150–180 m. For this time base the one-sigma precision is ~15 pptv and the estimated uncertainty is ±(15 + 6% of ambient mixing ratio) pptv. Ice particle concentrations were measured with a Cloud Imager Probe [*Baumgardner et al.*, 2002]. The tropopause altitude was determined in-flight with a Microwave Temperature Profiler (MTP) or from the aircraft soundings. Temporal information on storm development is available from the ER-2 aircraft Doppler Radar (EDOP) and Cloud Radar System (CRS) [*Heymsfield et al.*, 1996; *Li et al.*, 2004] and from the ER-2 Cloud Physics Lidar (CPL) [*McGill et al.*, 2002]. The ER-2 often flew on flight tracks directly above those of the WB-57F but at a higher altitude of ~20 km.

[13] The focus of CRYSTAL-FACE was not on the production of reactive nitrogen by Florida thunderstorms but on the radiative, microphysical, and chemical properties of cirrus clouds generated by deep convective systems or those formed in situ in the UT [*Jensen et al.*, 2004]. Flight tracks were therefore not designed to examine the entire altitude range of the thunderstorms. The WB-57F did not sample portions of anvils below ~10 km, i.e., anvil regions usually closer to the convective core(s), or the LT/BL region about the base of storms. There is no information from the program on the distribution of NO_x and quite limited information on the distribution of other chemical constituents in the LT/BL that fed the thunderstorms. Flash counts and location were available from the National Lightning Detection Network (NLDN). The NLDN counts were corrected for detection efficiency and, as also suggested by *Cummins et al.* [1998], weak positive flashes having a peak current less than 10 kA were subtracted from the total number of recorded flashes to yield the CG flash count. IC/CG ratios were determined from the climatology given by *Boccippio et al.* [2001]. For south Florida the mean ratio is in the range of 2–2.5 but the uncertainty in the number of

IC flashes calculated from the accumulated CG flashes for individual storms has to be considered large.

3. Altitude Distributions Within, About, and Above Thunderstorm Anvils

3.1. Influence in the Upper Troposphere

[14] Anvils from storms of a variety of sizes and lightning activity were examined, a few more thoroughly than others. Figures 1–3 give a summary of observations from 9 individual flights where the aircraft flew within the anvil outflow of storms at various altitudes or encountered NO due to upwind lightning activity. Minimum values of NO in the profiles are extrastorm air, and these mixing ratios are usually 100–200 pptv when below the tropopause. Peak mixing ratios of NO of only 1500 pptv within the anvil outflow would be a strong perturbation to local rates of ozone production or HO_x radical partitioning [e.g., *Pickering et al.*, 1996; *Jaeglé et al.*, 2000], yet 8 of 9 flights encountered elevated mixing ratios over broad horizontal regions greater than 3000 pptv and 4 of 9 flights exceeded 6000 pptv. The maximum mixing ratio of NO was near 9500 pptv. The apparent narrow peaks of NO in the profiles are the combined result of lightning activity and possible contributions from transport of NO_x from the LT/BL. NO_x from low altitudes should be nearly conserved during the short time (<1/2 hour) of transport to the anvil region and its partitioning would shift to favor NO depending upon the local temperature, ozone, and actinic flux as discussed previously.

[15] We emphasize that what appear to be narrow peaks or thin layers of NO in the altitude profiles of Figures 1–3 are broad regions covering many kilometers of enhancement usually observed while the aircraft flew at constant altitude through parts of an anvil. An example of the variability and scale of the enhancement encountered on a pass through the anvil or of storm-perturbed air is given for each flight in the panels to the right of the altitude profiles. The variability along a pass within the anvil can be large, a factor of 2–5, but not enormous which indicates that significant mixing occurred prior to the aircraft pass. Largest mixing ratios of NO were found on any pass within the ''thicker'' part of the anvil, indicated by the number concentration of ice crystals larger than 30 μm diameter included in the panels, or by the more dense regions readily identified in nadir images of the storms provided by the GOES satellite. There are exceptions where elevated NO was found in the absence of large ice crystals that, if formed, must have evaporated or suffered sedimentation. (A 30 or 100 μm diameter ice particle requires 9 or 0.9 hours to fall 1 km [*Jensen et al.*, 1994].) Examples are found at higher altitudes on flights 0719, 0721, and 0729 during anvil passes, and on flights 0726 and 0731 when the aircraft encountered high NO from previous or upwind thunderstorms. Thus there are cases where NO is a better tracer of the anvil outflow than the particle information or radar images.

[16] On the flight made on 0716 elevated NO was observed over a distance of ~25 km or over the distance covered within the anvil dimension identified by the ice crystal concentration (Figures 1c and 1d). On one of the passes through a much larger anvil on 0729 (Figures 3c and 3d) elevated NO larger than 4000 pptv with maximum mixing ratios near 9500 pptv was found over a distance of ~120 km. On 0728, where two passes were made at 13.5 km altitude within the anvil outflow of a highly electrically active storm, mixing ratios above 2000 pptv and as large as 7100 pptv were measured over a distance of 40 km (Figures 3a and 3b). There are also cases of sharp 2–4 s spikes in NO superimposed on the broader-scale enhancements, for example, near 70,500 s during the 0721 flight (Figure 2b). These spikes might imply that the aircraft was closer in time to IC activity within this storm. IC activity within the anvil region would take a longer time to mix within the rather nonturbulent outflow compared to discharges or portions of discharges that occurred within or nearer the core region where turbulent mixing would be greater. During the entire program, the pilots reported only two lightning flashes when flying within the anvil outflow. Thus it is not surprising that there are no examples of encounters with very large mixing ratios over short timescales (~1 s) that can be concretely attributed to nearby flashes like those reported by *Stith et al.* [1999] and *Huntrieser et al.* [2002]. In general, the relative behavior of NO within the Florida anvils was quite similar to that observed in previous studies of storms over New Mexico [*Ridley et al.*, 1996], over Europe [*Huntrieser et al.*, 1998, 2002], and over Colorado [*Dye et al.*, 2000]. An advantage of the present study was the ability to fly to higher altitudes, above storm tops, and into the lower stratosphere.

[17] The profiles as summarized in Figures 1–3 should not be misinterpreted. Below ~10 km, the profiles of NO are not those representative of lower altitudes about or within the storms but give the mixing ratio variation on ascent or descent closer to the Key West area. Between about 10 km and the tropopause there is a wide range of maximum mixing ratios and this range is very sensitive to where the aircraft flew within the anvil, especially to whether it transected regions closer to and above the storm core(s), and of course on the dynamics and accumulated lightning activity of the individual storms. For example, on the 0711 flight, 3–4 convective cells merged to form two separated anvils extending east to west over the southern tip of Florida. The northern storm sustained ~435 CG flashes and the southern storm ~257 CG flashes up to the time of the aircraft transects at the two altitudes given in Figure 1a. The transect across the northern anvil where NO reached maxima in the range of 5000–6500 pptv was at about 2/3 of the downwind distance of the visible anvil from the core region, while those in the southern anvil where NO was ~2000 pptv were nearer the end of the downwind anvil visible in the GOES images. On several flights (0723, 0728) the aircraft mostly probed the anvils well downwind of the core(s) or along the anvil edges and mixing ratios were correspondingly smaller. The well downwind portion of the anvil is air that was first convected to the UT and would have experienced the least lightning activity. Air parcels along the edge of the anvil would also have experienced greater mixing, dilution, entrainment with extra cloud air than air deeper within the anvil.

3.2. Influence of Upwind Thunderstorms

[18] Several flights illustrate the effect of upwind thunderstorms on the behavior of NO in the flight region. The

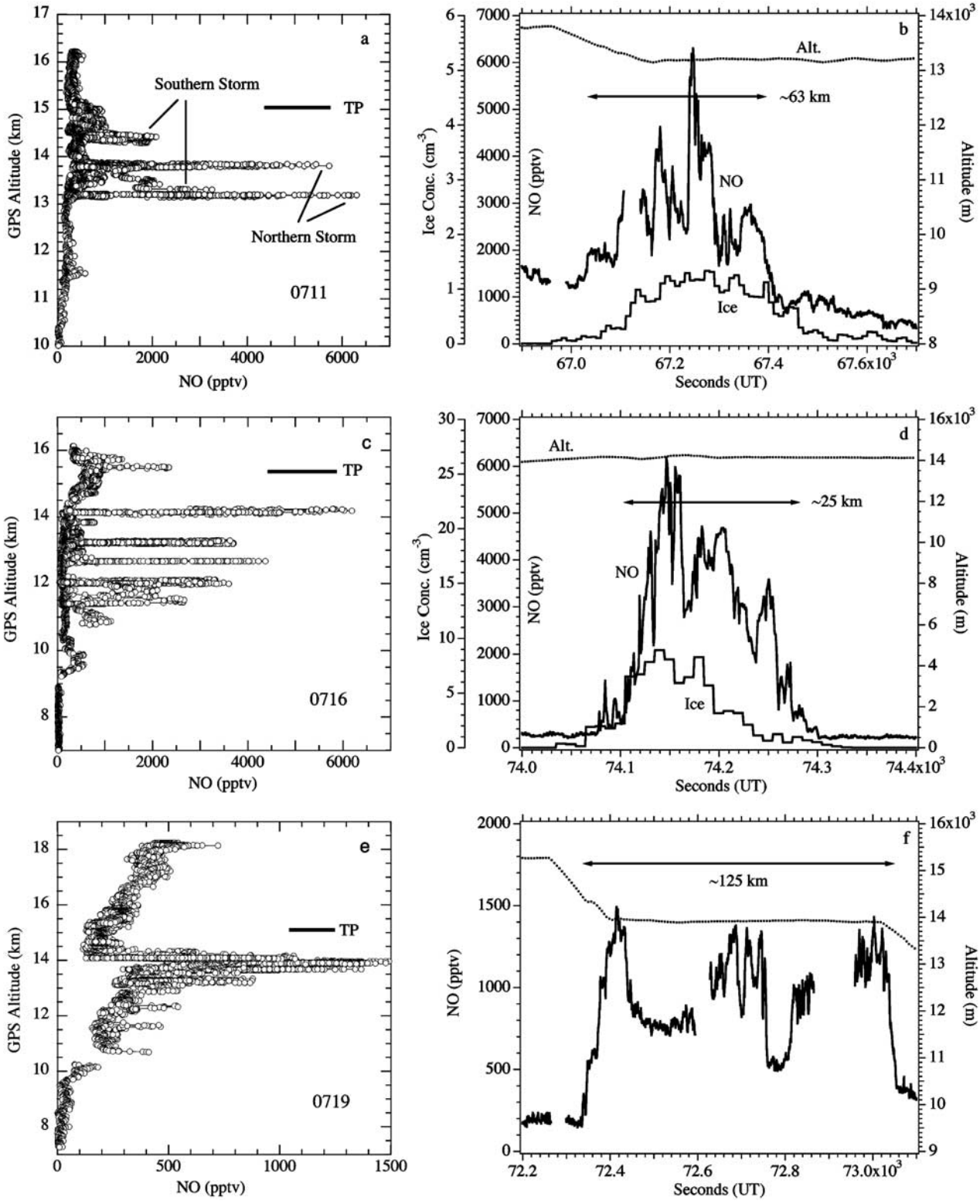

Figure 1. (left) Distributions of NO presented versus altitude. Apparent spikes of NO are from near-constant altitude transects of the anvils of active thunderstorms or from transects in clear air downwind of thunderstorm complexes. Below ~10 km the data are from ascents or descents closer to the Key West area, not in the vicinity of the thunderstorms studied at higher altitudes. (right) An example of a transect from each flight illustrating that the apparent spikes are large-scale enhancements. The 10-s concentration (cm^{-3}) of ice crystals larger than 30 μm diameter is included. Ice was not available on 0719. The *x* axis is seconds after midnight (UT). TP marks the lapse-rate tropopause altitude when well-defined.

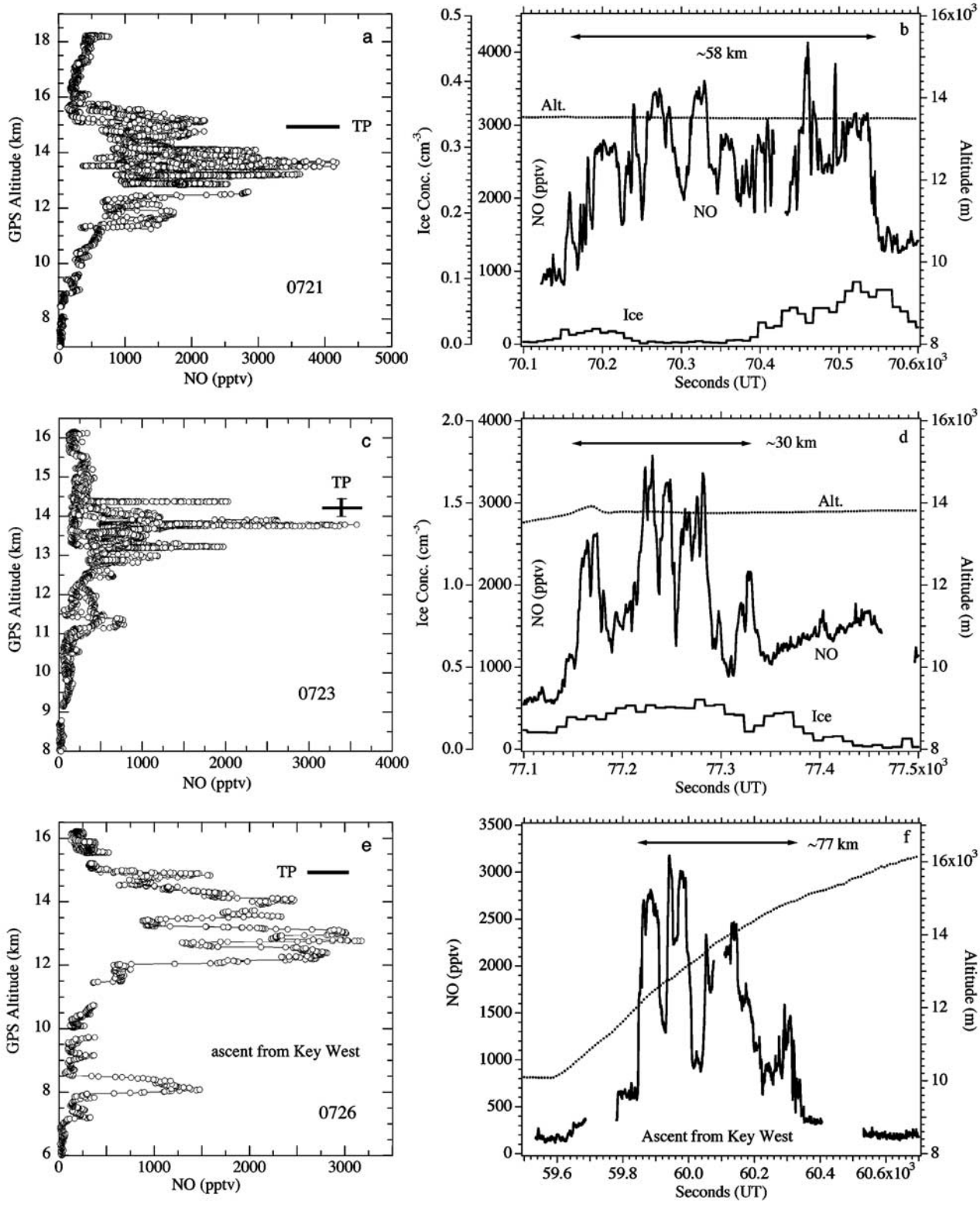

Figure 2. Same as Figure 1.

0721 flight is a striking case where extracloud mixing ratios of NO between 11 and 15 km are in the range of 600–1200 pptv, much larger than the 100–200 pptv more typical of extracloud or background air discussed earlier. On this flight, the vertical profile of Figure 2a is actually a composite of transects across the downwind portion of anvils of three separated storms that were aligned east to west and parallel over the west coast of southern Florida. Winds were from the NE to ENE at 7 m/s near 12 km and at 20 m/s near 14 km altitude. The three storms were rather small and lightning activity moderate (~215 CG flashes for all three storms during their ~2-hour lifetime). On initial

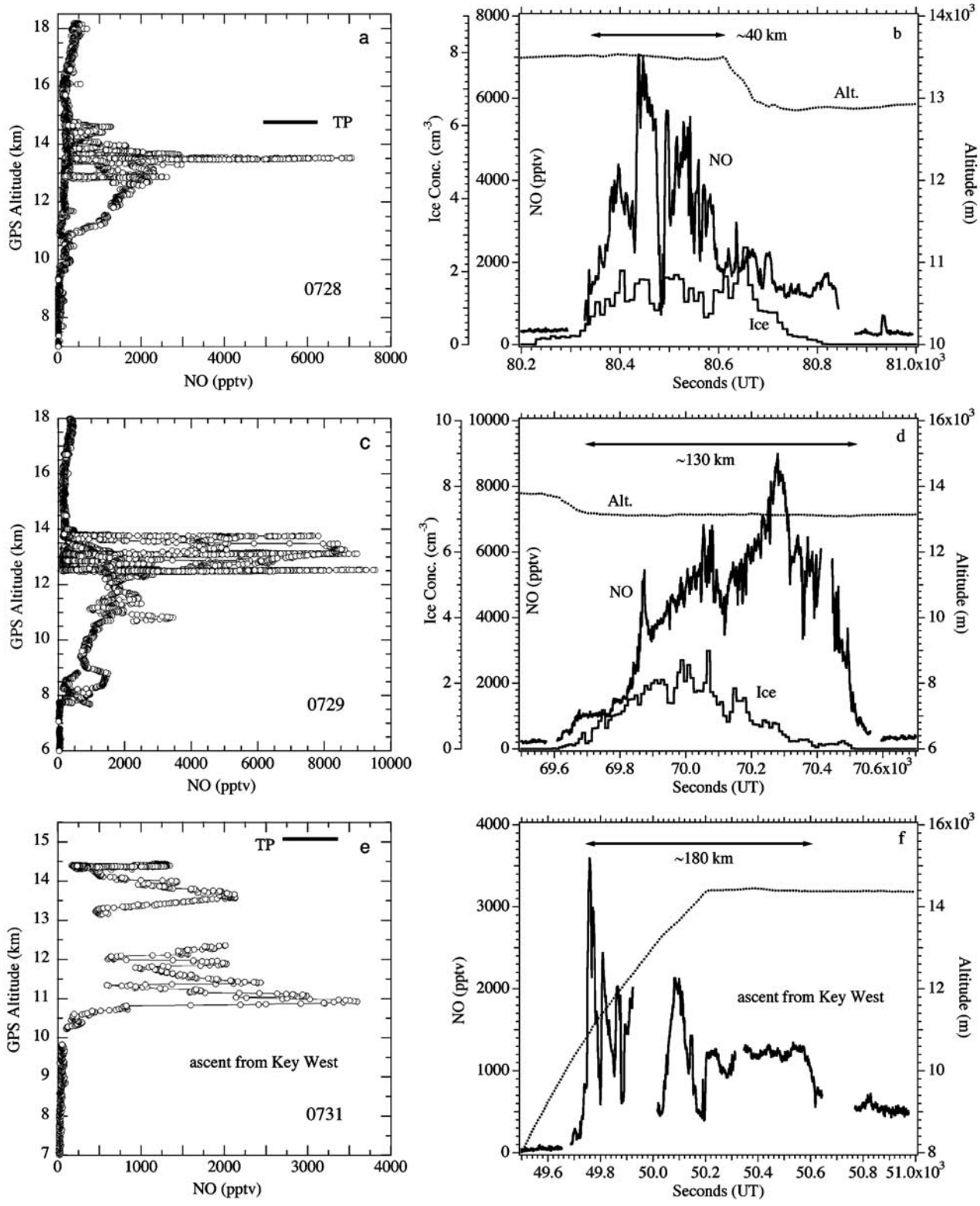

Figure 3. Same as Figure 1.

ascent the aircraft passed through the remnants of a previous storm anvil that had developed in the same region but had moved off the west coast of Florida and NO mixing ratios at this time were in the range of 1500–2000 pptv in cloud-free air. An examination of GOES images for the day showed that massive storms developed just off the east coast of Florida to the north east of the study region as well as to the north over the peninsula. These storms developed beginning about 0800 UT and decayed and regenerated throughout the day. Electrical activity was very high with more than 3000 CG flashes in the single storm complex to the northeast. By the end of the WB-57F flight the anvils of

all of these storms had merged into one giant layer covering the south Florida peninsula. However, the WB-57F did not examine this massive merged-anvil region but spent the last hour of the flight examining the lower stratosphere (LS) near 18 km. On descent from the LS the aircraft caught the downwind western edge of the complex between 14.7 and 11 km and NO mixing ratios up to ~2000 pptv were observed (Figure 2a). It is apparent that the high mixing ratios external to the anvils of the three smaller storms were the result of these storms being embedded in air already impacted by outflow from intense upwind lightning activity.

[19] Flights 0726 and 0731 are other examples of the influence of upwind electrically active deep convection influencing cloud-free regions of flight tracks. On 0726 the aircraft initially flew southwest from Key West before turning due south on its way to investigate the UT and LS region as far south as 12°N. Figure 2e shows that large mixing ratios near 3300 pptv were encountered on ascent between 12 and 15 km and over a horizontal scale of 77 km. Winds were light at 4–8 m/s but from the direction of a large storm complex off the north coast of Cuba and due south of the Florida peninsula. The complex was present by 0500 UT, well before the flight started near 1600 UT, and persisted until about 2030 UT. On 0731, the aircraft climbed in cloud-free air and headed north from Key West along the west coast of the Florida peninsula and encountered large mixing ratios up to 3600 pptv between 10 and 14.5 km, or to altitudes not far below the local tropopause, which was located near 15.2 km. Elevated NO was observed over a horizontal distance of ~180 km (Figure 3f). GOES images revealed that large areas of deep convective complexes covered most of the Florida Keys and ocean regions to the west and southwest as well as the entire southern portion of the peninsula from at least 0000 UT to 0700 UT. Residual smaller cells remained until 0830 UT. Flow was from the southwest at 4–7 m/s above 10 km. Takeoff did not occur until near 1300 UT, but residual high NO from the deep convection was encountered.

3.3. Influence in the Lower Stratosphere

[20] Included in Figures 1–3 is the lapse-rate tropopause altitude, when well defined, in the region of the storms determined by the MTP instrument or from the aircraft temperature data when ascents or descents occurred near the anvil region. On 0729 a double tropopause was present: a strong inversion occurred near 15.8 km and a very weak inversion that was penetrated by the convection (see Figure 3c) occurred near 13.2 km. The radars and lidar onboard the ER-2 aircraft revealed no cloud tops or convective bubbles above the well-defined lapse-rate tropopause for any of the storms investigated by the WB-57F. An examination of the left panels of Figures 1–3 shows that there was only weak enhancement of NO above the tropopause on the flights of 0716 and 0721. Although all of the storm tops as measured by enhanced NO reached similar altitudes of 14–15 km, with influence up to very near the tropopause in individual cases, the vertical distributions of maximum NO mixing ratios show that the major injection of NO occurred starting 1 or 2 km below the local tropopause.

[21] Above the tropopause the mixing ratios given in Figures 1–3 can represent regions also distant from the storm anvils under study, although in nearly every flight an excursion into the lower stratosphere was made above or close to the anvil outflow. Most flights have more than one ascent/descent into/from the lower stratosphere. The range of NO mixing ratios that was observed above the local tropopause was much smaller than below on all but the 0721 flight. Since on many flights there were also storms upwind of the track of the WB-57F, the uniformity of the lower stratospheric mixing ratios on any flight also argues against significant widespread injection of enhanced NO above the tropopause.

[22] This compact behavior in the lower stratosphere is illustrated in Figure 4, which gives a composite of the NO mixing ratios from the 9 thunderstorm flights with potential temperature (Θ) as the vertical coordinate. There was no enhanced NO above ~370 K, NO was quite uniform at larger Θ. Largest NO mixing ratios were found in the outflow between 345 and 360 K, the lower Θ of 345 K being determined here by the WB-57F not having probed anvils below about 10 km altitude. The tropopause Θ, determined for the lapse-rate tropopause by MTP in the vicinity of the storms, ranged from 355 to as high as 380 K, the latter only during the first part of the flight of 0731. Excluding the 0731 flight the range was 361–365 K. There are smaller enhancements of NO above the average of 363 K on two of the nine flights: 0716 and 0721. Whether this indicates some injection into the lowest stratosphere depends on the choice of the precise definition of the tropopause. What is clear is that the bulk of the lightning-generated NO or LT/BL transported NO_x was injected into the UT.

4. Estimates of NO_x Vented to the UT

[23] Only two isolated storm systems (on 0716 and 0729) of quite different size and electrical activity were examined sufficiently well by the WB-57F to allow an approximate estimate of the total mass of NO_x produced by lightning flashes, plus any transported from the LT/BL, that is vented to the UT.

4.1. Storm Investigated on 0716

[24] On 0716 a storm started to develop near 1900 UT over southern Florida. The anvil outflow was fed by ~9 individual cells during the first hour (E. Zipser, private communication, 2003). By 2200 UT most of the anvil outflow had moved off the west coast over the Gulf of Mexico. The WB-57F probed the anvil outflow quite extensively over the altitude region of 11.4–14.2 km (Figure 1c) between ~2030 and ~2230 UT by making 3 diagonal passes over and near the core region and 4 longitudinal passes within the downwind anvil. Examples of a diagonal and a longitudinal pass are shown superimposed on GOES visible images in Figure 5. After the last longitudinal pass the aircraft ascended into the lower stratosphere to ~16 km and immediately descended to further probe the anvil outflow for another 10 min.

[25] The temporal development of the storm is shown in Figure 6, which gives radar reflectivity cross-sections obtained from either the EDOP or CRS instruments while the ER-2 was flying near 20 km altitude and along longitudinal tracks over the southern half of the outflow. East-to-west or west-to-east ER-2 tracks moved with the

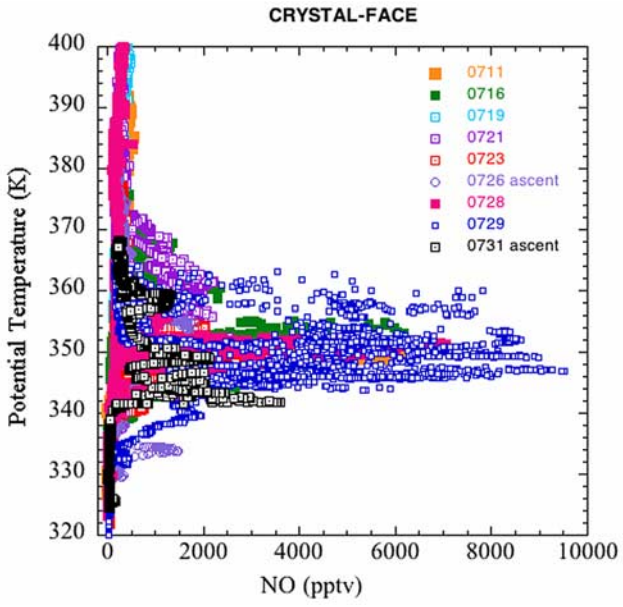

Figure 4. A summary of the distributions of NO plotted against potential temperature. The data extend uniformly to 435 K (not shown).

westward translation of the storm but were near and above the track shown for the WB-57F in Figure 5b. Because the storm translated west and the anvil expanded some with time, the radar scans do not cover exactly the same portion of the storm on successive passes. Scans from nearly parallel tracks ~25 km to the north showed that the anvil outflow was weaker to the north and that the anvil top sloped downward by 1–1.5 km over a distance of 25–30 km.

[26] The 2016–2030 UT EDOP scan shows that the convection initially reached ~15 km altitude and that the anvil covered ~100 km downwind at altitudes above 10 km. Both the MTP data and the aircraft soundings indicated that the tropopause was at 15.2–15.4 km in the vicinity of the storm or that the core convection was effectively capped by the temperature inversion. The 2126–2140 UT CRS scan shows precipitation in the core region that weakened significantly by 2200 UT. Indeed no strong updraft regions remained in the core EDOP or CRS doppler velocity retrievals after ~2100 UT (not shown). The last scan shown (2242–2249 UT) was taken ~20 min after the WB-57F made the final longitudinal pass and shows that the "particle" anvil along the southern side of the GOES image was mostly confined to 9–14 km altitude. Of course the distribution of gaseous reactive nitrogen could cover a larger vertical area than is depicted by the radar images due to evaporation or sedimentation of hydrometeors.

[27] Table 1 shows the accumulated CG activity derived from the NLDN data. Lightning started between 1900 and 1915 UT and nearly ceased by 2100 UT consistent with the lack of strong updrafts in the core region near this time from the radar data. Allowing ~1/2 hour for vertical transport from low altitude to the anvil region, ~90% of the CG activity occurred before the WB-57F made the second diagonal pass through the anvil near 2052 UT so there was little further input of CG-produced NO or LT/BL-transported NO_x to the anvil outflow. We have no information on possible IC activity after this time other than the lack of any observations of flashes by the pilots. Thus with the disappearance of significant updrafts after ~2100 UT the investigation of this anvil was unique and allows a reasonable estimate of the NO_x content to be made.

[28] Independent of the radar scans, the distribution of NO in the anvil outflow region was well mapped by the aircraft. The NO mixing ratios observed for the first diagonal pass made at 14.2 km altitude are given in Figure 1d. Maxima in the range of 2000–6500 pptv were recorded over a distance of 25 km. Data from the longitudinal pass of Figure 5b made at 12.0 km altitude are given in Figure 7. As the aircraft entered cloud from east to west, higher NO (2000–3500 pptv) occurred in the upwind region over a distance of 29 km, similar to the behavior and scale observed during the diagonal passes, and then lower more uniform enhancement (500–800 pptv) occurred over a

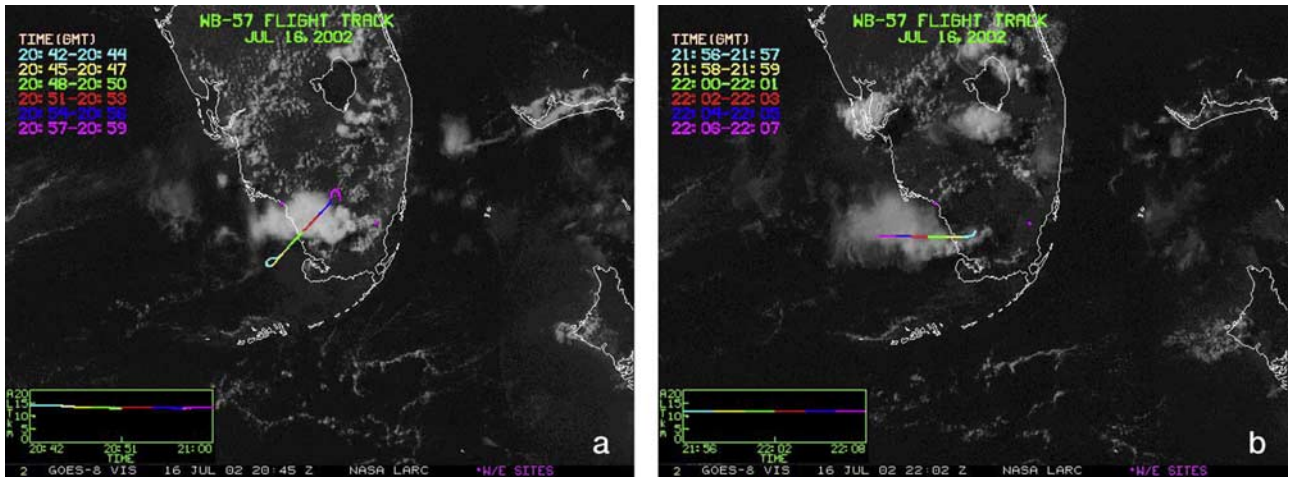

Figure 5. The storm investigated on 0716 with examples of an (a) diagonal and (b) longitudinal transect superimposed on false-color visible GOES images. The longitudinal pass extended in a straight line west beyond the visible anvil. For reference, the distance across the peninsula through the southern part of Lake Okeechobee (located to the NNE of the storm) is ~220 km.

Table 1. CG Flashes for the Storm of 0716[a]

Time, UT	Accumulated CG Flashes
1930	23
2000	202
2030	345
2100	382
2200	392

[a]Lightning started near 1900 UT.

distance of 48 km until the aircraft exited the downwind anvil at 79880 s. The decrease in elevated NO on both the longitudinal and diagonal passes correspond well to the edges of the clouds seen in the GOES images or the radar scans. The downwind anvil reflects air that was transported vertically during the early stages of the storm development and air likely exposed to less electrical activity. Table 2 summarizes the median mixing ratios of NO in the in-anvil passes and shows that the relative behavior was quite consistent at each altitude. With the exception of pass 4, the upwind anvil (eastern end) contained larger NO over a distance of 24–29 km; the downwind region contained lower NO over a distance of 46–57 km. (Track lengths in parentheses in the table were from nonlinear passes that do not allow a definition of the scale of the high and low NO regions.) Pass 4 was made along the southern edge of the anvil sometimes in and sometimes out of the anvil outflow. The table summarizes the mixing ratios for the in-anvil portions of this track and shows that in the upwind anvil median mixing ratios closer to the southern edge were lower than those of pass 5 that was made in the thicker part of the anvil to the north. Pass 8 was a circular track within the upwind anvil at 12.0 km altitude and although almost an hour later gave a comparable mixing ratio to that observed in the upwind portion of pass 5. Pass 9 was a short extension of pass 8 that descended out of the anvil edge but serves to show that elevated NO was observed down to at least 11 km altitude.

[29] To estimate the amount of NO_x contained within the anvil outflow we approximated the outflow as an upwind circular region of higher NO of diameter 25 km, and a rectangular downwind region of lower NO of length 50 km and width 15 km for each of the altitude bins shown in Table 3. Although the GOES nadir image and the scans from the ER-2 radars show the outflow width was on average 25–30 km we have chosen a narrower 15 km width to allow for a decrease in mixing ratios as the northern and southern storm edges are approached. At this stage of analysis the focus is on a conservative lower estimate of the NO_x content. Table 3 summarizes the results for the total number of molecules of NO_x for each altitude bin centered around the pass altitudes for the "high" and "low" NO regions. NO_x was estimated from NO using clear sky J-values and the average O_3, temperature, and pressure for each pass as discussed in section 1. If J was reduced within anvil from the clear sky value by a factor of two the NO_x content would be increased from that given by only 15–20%.

[30] The lower limit estimate of the total NO_x vented to the UT above 10 km is 42×10^{27} molecules. If we consider the midtime of the WB-57F anvil passes (2130 UT) then the second panel of Figure 6 shows considerable portions of the anvil below 10 km. If this storm cross-section is used to define the anvil and convective core region down to 6 km, and mixing ratios as large as 1000–2000 pptv of NO_x are assumed, then this lower portion of the anvil would contain $11–22 \times 10^{27}$ molecules of NO_x or ~25–50% of that estimated for above 10 km. Considering that *Langford et al.* [2004] have recently reported NO_x mixing ratios of ~3000 pptv in the updraft of a Colorado thunderstorm, we consider that an upper limit would be a factor of two larger than our estimate for above 10 km or that $42–84 \times 10^{27}$ molecules of NO_x (980–1950 kg(N)) is a reasonable range

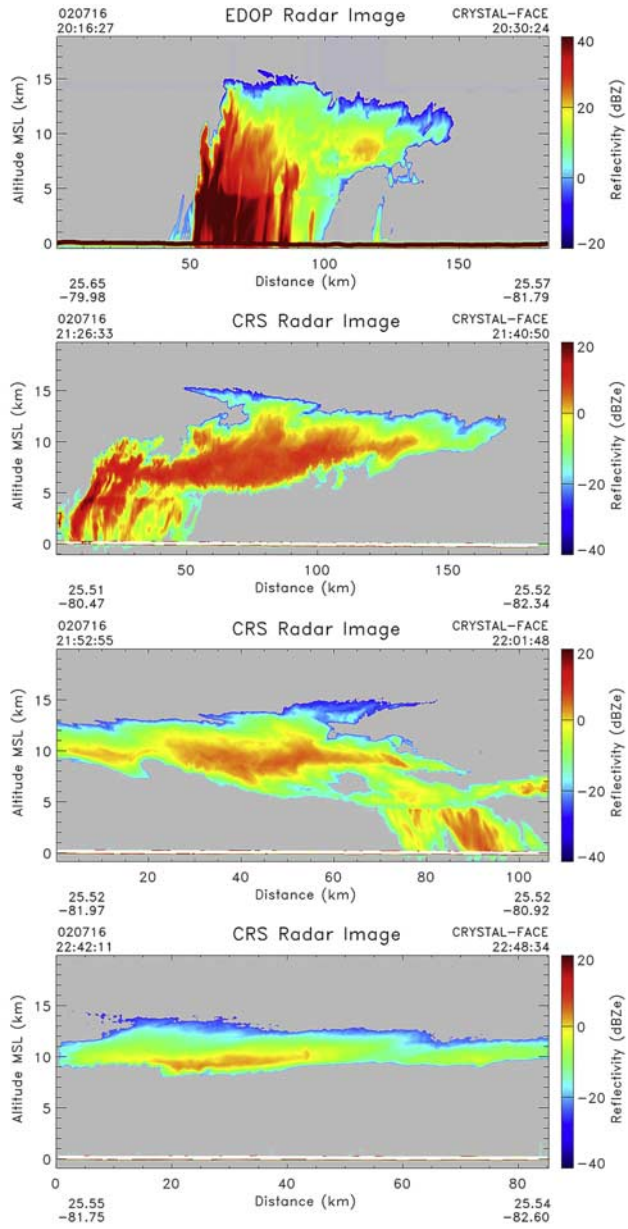

Figure 6. The temporal development of the 0716 storm illustrated by radar reflectivity measured by the ER-2 EDOP and CRS instruments. These images are from ER-2 longitudinal passes over the southern half of the anvil and above that of the WB57-F pass that is shown in Figure 5b. The ER-2 traveled east to west in the top two and bottom panels, and west to east in the remaining panel. The WB-57F probed the anvil from ~2030 to 2230 UT.

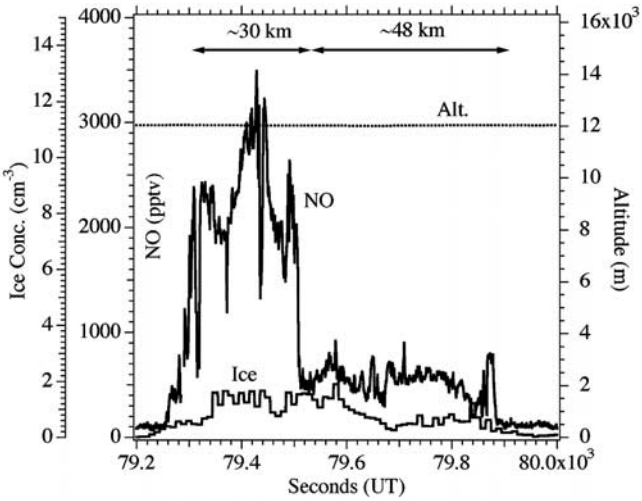

Figure 7. NO and ice particle data from the longitudinal pass of Figure 5b, made at 12 km altitude, showing the high and low NO regions of the anvil.

for the total content above 6 km. To put this total into perspective, it is approximately equivalent to the exhaust emissions of NO_x from a Boeing 757 aircraft operating at cruise altitude for 75–150 hours [*Brasseur et al.*, 1998b].

[31] We stress that the estimate of total NO_x represents the combined production from IC lightning, from lightning (IC and CG) within the core that is transported to the anvil, and any NO_x transported from the LT/BL. It is not the total produced by all lightning activity because (1) we have no information on mixing ratios of reactive nitrogen at lower altitudes generated by portions of CG discharges external to the convective core, or of the amount (if any, see section 6) that is carried to low altitudes by downdrafts. However, in this case where the aircraft examined the anvil mostly after CG lightning and strong updrafts and downdrafts had ceased, it is unlikely that large amounts of NO_x originally within the core updrafts were missed in the summation. In contrast, the estimate of total NO_x will be larger than that just produced by lightning activity because of (2) unmeasured contributions from transport of NO_x from the LT/BL. However, if we make the unlikely assumption that the enhanced mixing ratios of NO in the "low" NO rectangle of Table 3 are all due to transport from the LT/BL and that those mixing ratios should be subtracted from the medians found in the "high" NO circular area to obtain just the contribution from lightning production of NO, then the low end of the estimated range would be reduced by less than 50%. Because these factors 1 and 2 offer some compensation, it is considered that the estimate of $42-84 \times 10^{27}$ molecules of NO_x is a reasonable range for the NO_x produced by just lightning activity, but admit that it could be high by no more than a factor of 2.

Table 2. Summary of Anvil Passes by the WB-57F for the 0716 Storm

Pass	Type	Midtime, UT	GPS Altitude, km	Track Length, km	Median NO, pptv
1	diagonal	2037	14.2	24.5	3317
2	diagonal	2052	13.2	24	2497
3	diagonal + circle	2109	13.2	(51)	2068
4	longitudinal (E→W)	2120	12.7	(14)	1303
				(17)	1886
				(13)	952
5	longitudinal (W→E)	2145	12.7	46	805
				24.5	2305
6	longitudinal (E→W)	2206	12.0	29.3	2096
				48	587
7	longitudinal (W→E)	2226	11.4	57	362
				28	830
8	circle (E end)	2255	12.0	(53)	1945
9	semicircle, descent	2302	12.0–11.1	(16)	1282

Table 3. Estimate of NO_x Content in the 0716 Anvil Outflow

Altitude Bin, km	25 km Diam. "High" NO Circle		15 km × 50 km "Low" NO Rectangle	
	Median NO, pptv	Molec. $NO_x/10^{27}$	Median NO, pptv	Molec. $NO_x/10^{27}$
14–14.5	3317	4.8		
13–14	2283	7.4		
12.5–13	2305	4.1	805	2.2
12–12.5	2096	4.3	587	1.8
11–12	1056[a]	5.0	362	2.6
10–11	1282	6.7	362[b]	2.9
Total		32.3		9.5

[a]Average of the medians of pass 7 and pass 9, Table 3.
[b]Assumed.

[32] Within these uncertainties the average production of NO per lightning flash, P, can be estimated. We also have to assume that the climatological IC/CG ratio of 2–2.5 for south Florida [*Boccippio et al.*, 2001] is applicable to this storm. With 392 CG flashes, ~882 (2.25 × 392) IC flashes are estimated. Two choices can then be made. The first, based on evidence summarized in the introduction, is to consider that IC and CG flashes are equally efficient in NO production, i.e., P(IC) = P(CG) = P, which yields a production per flash of $P = 0.33-0.66 \times 10^{26}$ molecules NO/flash. Using 44 s^{-1} as the average global flash rate [*Christian et al.*, 2003], a bold extrapolation of this single storm to represent the global production would yield 1.1–2.2 Tg(N)/yr. Given the complexity and variety of thunderstorms, the worth of such an extrapolation is low.

[33] The second approach is to make the more usual but possibly invalid assumption that P(IC) = 0.1P(CG). Then P(CG) for the 0716 storm ranges from $0.88-1.8 \times 10^{26}$ molecules NO/flash, and this range is much less sensitive to any uncertainty in the IC flash count. This P(CG) estimate is lower than the value of $P(CG) = 6.7 \times 10^{26}$ molecules NO/flash that was recommended by *Price et al.* [1997a] and is used in many CTMs. Comparing a single storm with climatology is of course arguable, but our estimate of P(CG) for this storm is at least a factor of 4 smaller considering that we cannot account for the amount of NO_x transported to the anvil from the LT/BL. Within the assumption that IC flashes are 1/10th as efficient, our P(CG) estimate is more in line with the value of 2.0×10^{26} (range $0.77-3.8 \times 10^{26}$) molecules/CG flash derived from a supercell storm over Germany [*Fehr et al.*, 2004], but considerably smaller than the estimate of $(5.8 \pm 2.9) \times 10^{26}$ molecules/CG flash derived by *Langford et al.* [2004] from observations of a thunderstorm over Colorado.

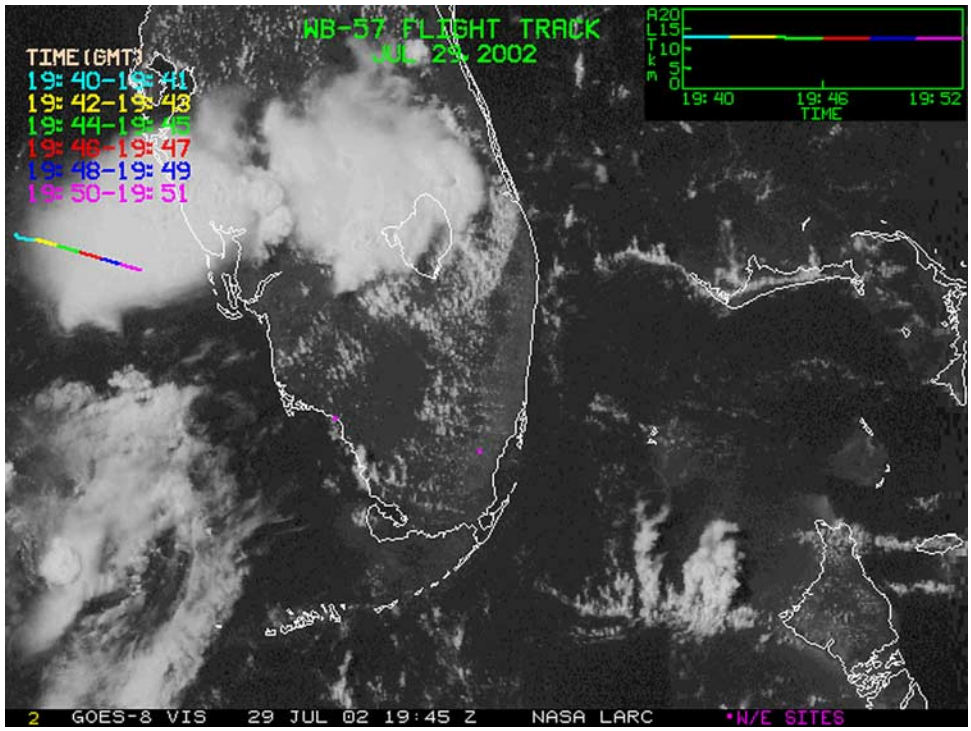

Figure 8. GOES image showing the WB-57F pass through the 0729 storm anvil while at 12.5 km altitude. The aircraft turned around within the anvil at the end of this pass. The distance across the peninsula through the southern end of Lake Okeechobee is ~220 km. After the aircraft left the storm to return to base, the anvils of the two systems shown in the figure merged to form a very large anvil complex. Both storms remained electrically active after the aircraft departed.

4.2. Storm Investigated on 0729

[34] On 0729 a large and very electrically active storm was investigated as shown in the GOES image for 1945 UT in Figure 8. The storm started near 1700 UT, at least two convective cells contributed to the anvil prior to investigation, and the anvil increased in plan area by a factor of 1.5 between 1925 and 2011 UT, the period of in-anvil investigation by the WB-57F aircraft. A total of 3067 ± 150 CG flashes occurred up until the aircraft stopped examining the storm: 339 by 1800 UT, 989 between 1800 and 1900 UT, and 1739 between 1900 and 2000 UT. (The uncertainty of ±150 flashes is due to ambiguity in assigning the flashes to the storm under investigation versus the second system to the northeast that is shown in Figure 8.) The accumulated number of CG flashes to the time of aircraft departure was a factor of 8 larger than occurred in the 0716 storm, and the 0729 storm remained active after the aircraft departed to return to base. Superimposed on the GOES image for 1945 UT is one of three similarly located tracks made by the WB-57F between 12.5 and 13.2 km altitude. This flight track actually extended farther in a straight line from that shown but the aircraft turned around before reaching the southeastern edge of the outflow. NO data from this pass and the remainder of the flight within or near the anvil are shown in Figure 9. Mixing ratios above 2000 pptv and as high as 9500 pptv were recorded within the anvil on these passes. The median NO mixing ratio for the pass at 12.5 km shown by the shaded bar in Figure 9 was 4375 pptv. Figure 3d shows the data from another pass made at 13.2 km essentially along the same track as shown in Figure 8. Elevated NO with a maximum near 9000 pptv was recorded over a distance of ~130 km within the anvil. The median mixing ratio was 4450 pptv. A third pass also at 12.5 km had a median mixing ratio of 3388 pptv. As shown in Figure 9, the aircraft climbed within the anvil to just above the anvil top. Large mixing ratios up to 8200 pptv were observed up to the cloud top height of 13.8 km, determined

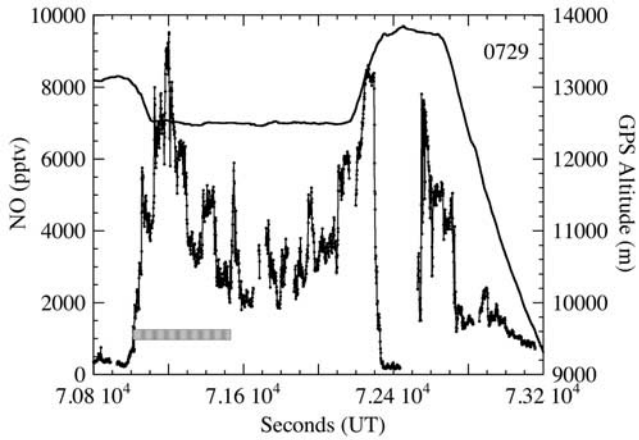

Figure 9. NO mixing ratios observed during the pass (indicated by the shaded bar) shown in Figure 8. The aircraft then turned around within the anvil, headed NW, climbed within and exited the cloud top near 72,300 s, and reentered the anvil on descent near 72,500 s.

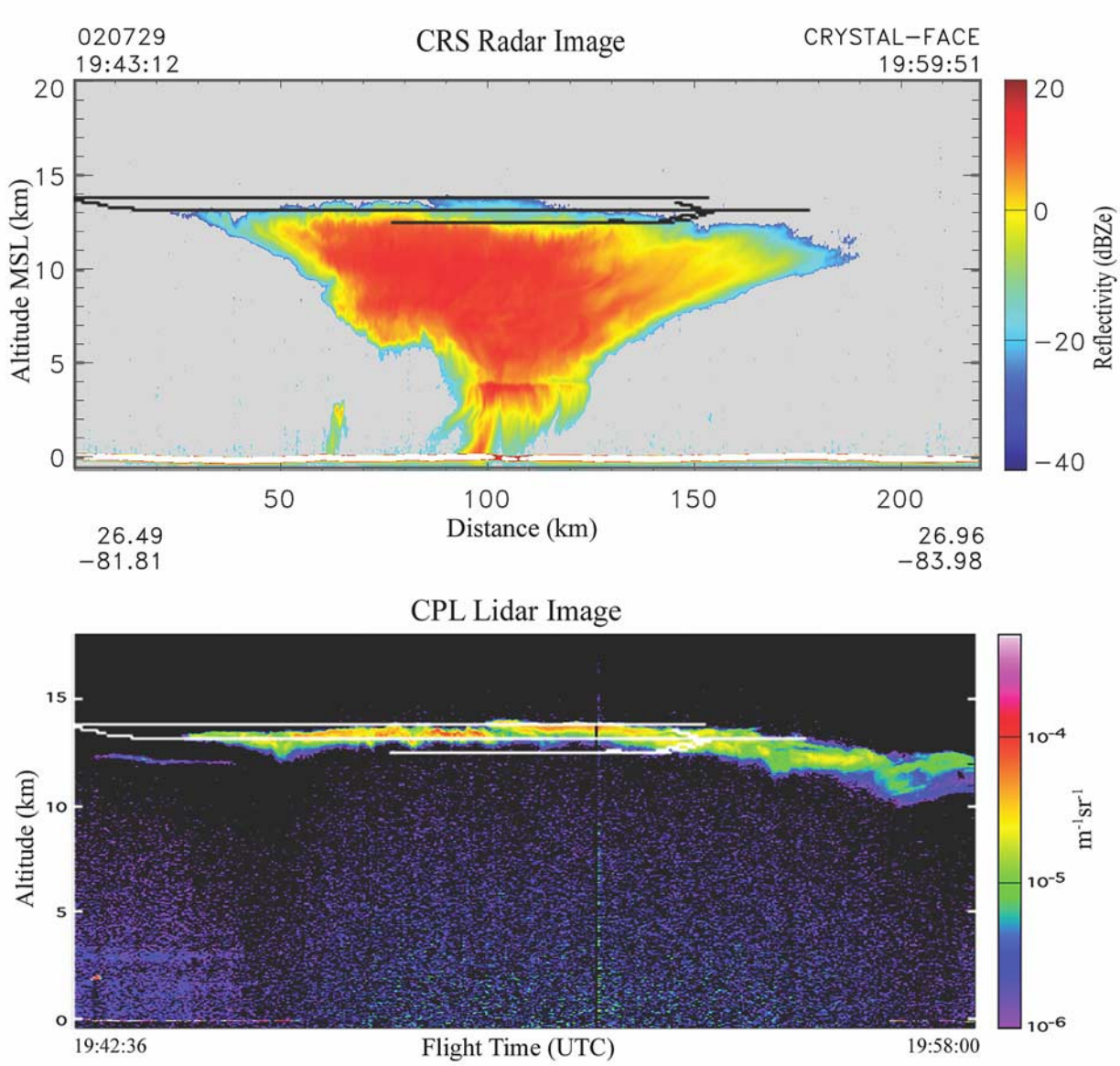

Figure 10. Cloud Radar System reflectivity cross section of the 0729 storm measured from the ER-2 aircraft along a track directly above that of the WB-57F aircraft track shown in Figure 8. All of the WB-57F transects (black lines in the upper panel and white lines in the lower panel) in the upper part of the anvil were made between 1925 and 2011 UT. Data from the CPL instrument (bottom panel) also on the ER-2 show the altitude extent of the upper anvil more sensitively.

by the large drop in NO or ice particle concentration (not shown), and on the descent back into the anvil.

[35] Figure 10 shows the CRS radar and CPL lidar cross-section of the storm at ~1950 UT obtained from the ER-2 flying at 20 km altitude along a track directly above that of the WB-57F track shown in Figure 8. The anvil cross-section above ~8 km is quite symmetric in both radar reflectivity and shape with an anvil dimension at its widest point of ~130 km. The figure includes the tracks of the WB-57F, the last pass by the aircraft occurred ~15 min after this cross section was obtained. Neither the ER2 nor WB-57F tracks passed over the thicker convective core region that was more to the east and it was unfortunate that the WB-57F did not have fuel to examine the lower altitude and higher radar reflectivity regions of this classic-looking storm.

[36] Because of the very limited altitude range of the sampling it is not possible to estimate the total amount of NO_x within the storm due to lightning activity and/or LT/BL influx as reliably as for the 0716 storm. Considering the symmetry of the radar image we have some confidence in estimating the amount above 10 km altitude by dividing the radar image into circular layers, the diameter determined from the cross section given in Figure 10. We assumed that the median mixing ratio for the 10–11 and 11–12 km layers was 4300 pptv, nearly the same as measured for the 12–13 km layer. As in the 0716 case, measured temperatures, pressures, and in-cloud ozone were used to determine

Table 4. Comparison of the 0716 and 0729 Storms

	0716	0729
GOES plan area,[a] km^2	~4200	~15,000
Molecules of NO_x	$4.2–8.4 \times 10^{28}$	$170–230 \times 10^{28}$
Tons, N	0.98–1.95	40–53
CG flashes	392	3067 ± 150
Mean CG peak current,[b] kA	−25.7	−19.5
IC flashes from climatology	~882	~6900
P molecules NO/flash	$0.33–0.66 \times 10^{26}$	$1.7–2.3 \times 10^{26}$
P(CG) molecules NO/CG flash	$0.88–1.8 \times 10^{26}$	$4.5–6.1 \times 10^{26}$
Tg(N)/yr based on 44 flashes s^{-1}, P	1.1–2.2	5.5–7.5
Maximum altitude, km	15.2	13.8
Lightning duration, hour	~2	~3[c]
Average CG flash rate, min^{-1}	~3	~17

[a]Area near the time of aircraft departure.
[b]Mean current of the dominant negative CG flashes.
[c]The duration is considered only to the time of aircraft departure.

molecular densities and the NO_2/NO ratio. The result for the content between 10 and 13.8 km is 10×10^{29} molecules of NO_x or 23×10^3 kg(N) and is considered a good lower limit to the total content of the storm.

[37] It is possible to determine some rough bounds on the total storm content above 5 km altitude. Assuming that all layers below 10 km sustained median mixing ratios of NO_x of 4000 pptv, approximately the same as above 10 km, the content from 5–10 km would be an additional 13×10^{29} molecules. Based on previous storm studies in New Mexico, Colorado, and Europe, where there was a tendency for larger mixing ratios to be found in the upper half of the anvil, a tendency also seen in Table 3 for the 0716 storm, mixing ratios of 1/2 this scenario are likely more reasonable. Thus the estimate of the total storm content is $17–23 \times 10^{29}$ molecules ($40–53 \times 10^3$ kg (N)) or 21–54 times that determined for the 0716 storm. The higher end of the range could be low for the same reasons described for the 0716 storm, namely production of NO by portions of flashes external to the storm or possible transport from the storm by downdrafts. Similarly, the contribution by transport from the LT/BL is unknown. In this case, however, the observed median mixing ratios in the upper portion of the anvil were a factor of 2 larger than in the 0716 storm. Thus, if we make the unlikely assumptions that the median LT/BL NO_x mixing ratio was as high as 1000 pptv and that it was transported undiluted to the anvil region, then the lower end of the range now attributable to just lightning production would be reduced by only ~25%. Again, because of compensation between these factors, we consider that the range of $17–23 \times 10^{29}$ molecules a reasonable estimate of the production by just lightning activity.

[38] Table 4 shows that the larger storm of 0729 obviously released a much larger mass of reactive nitrogen to the middle and upper troposphere than the 0716 storm. The average CG flash rate was ~6 times larger and the accumulated CG flash count was ~8 times larger in the 0729 storm. The derived values of P, P(CG), or global yearly production differ in the midpoint of the range by a factor of 4 and the full range is a factor of 7. A factor as large as 4–7 clearly demonstrates that individual storm systems differ greatly in both the mass of reactive nitrogen produced and in the derived quantities. For example, and in sharp contrast to the result from the 0716 storm, the estimate of P(CG) from the 0729 storm is only slightly smaller than the recommendation of P(CG) = 6.7×10^{26} (range $3–10 \times 10^{26}$) molecules of NO/CG flash by *Price et al.* [1997a] although the mean current of the dominant negative flashes was larger for the 0716 storm.

[39] Our estimates of P, and to a lesser extent P(CG), are clearly sensitive to the IC/CG ratio assumed for the storms and there is indirect evidence that the IC activity for the 0729 storm was much larger than assumed from climatology. On 0716 the fraction (F) of weak positive discharges having a peak current less than 10 kA was only 0.08. The average F for all NLDN flashes over the entire month of July was 0.11. In contrast, up to the time of aircraft departure on 0729, a much larger F = 0.33 was recorded. If these weaker discharges are interpreted as IC flashes, as suggested by *Cummins et al.* [1998], then the proportion of IC activity was ~4 times larger on 0729. Assuming that the July average F was representative of the climatological IC/CG ratio of 2.25, then the IC/CG ratio for the 0729 storm would be ~7. With this IC/CG ratio the estimates of P and P(CG) for the 0729 storm given in Table 4 would be reduced to $0.69–0.94 \times 10^{26}$ and $3.3–4.4 \times 10^{26}$ molecules NO/flash, respectively. Thus, although the range of estimates of the mass of reactive nitrogen from the aircraft observations of the two storms is considered to be reasonable, the lack of measurement of the IC activity during the experiment makes the derived quantities for the 0729 storm more uncertain.

[40] Table 4 also shows that the average flash rates for the two storms do not scale as $\sim H^5$, where H is the cloud top altitude, as has been suggested to occur from some climatological analyses [*Price and Rind*, 1992, and references therein; cf. *Molinié and Pontikis*, 1995; *Ushio et al.*, 2001]. Both storms also generated comparable maximum updraft velocities: 0716 at 26 m/s and 0729 at 24 m/s [*Siewert et al.*, 2003]. Another example is a smaller storm investigated on 0719 that reached 13–14 km altitude, an altitude comparable to the cloud tops of 0716 and 0729, but only 10 CG flashes were generated and maximum mixing ratios of NO within the outflow were only ~1500 pptv (Figures 1e and 1f).

5. Comparison With the MOZART-2 CTM

[41] In this section a comparison of the lightning parameterization used in MOZART-2 [*Horowitz et al.*, 2003] is made with the aircraft and NLDN observations for the month of July 2002. Figure 11 shows the 9 grid points of the model, each marked by a star, chosen for comparison with the observations. At T42 resolution (~280 km in longitude, ~320 km in latitude), only 3 grid points or cells (labeled 1, 2, and 5) represent most of the land area of Florida. The model parameterizes the total flash rate, IC/CG partitioning, and production per flash type according to the recommendations of *Price and Rind* [1992, 1994] and *Price et al.* [1997a]. It also includes their suggested scaling to account for differences in model resolution. For a given cloud top height H (km), the total (IC + CG) flash rate for continental locations is much larger than for marine locations: $F_{cont} = 3.44 \times 10^{-5} H^{4.92}$ min^{-1}, while for maritime storms, $F_{mar} = 6.40 \times 10^{-4} H^{1.73}$ min^{-1} [*Price and Rind*, 1992]. The production per CG flash of 6.7×10^{26} molecules NO/CG flash and 1/10 of that for IC flashes proposed

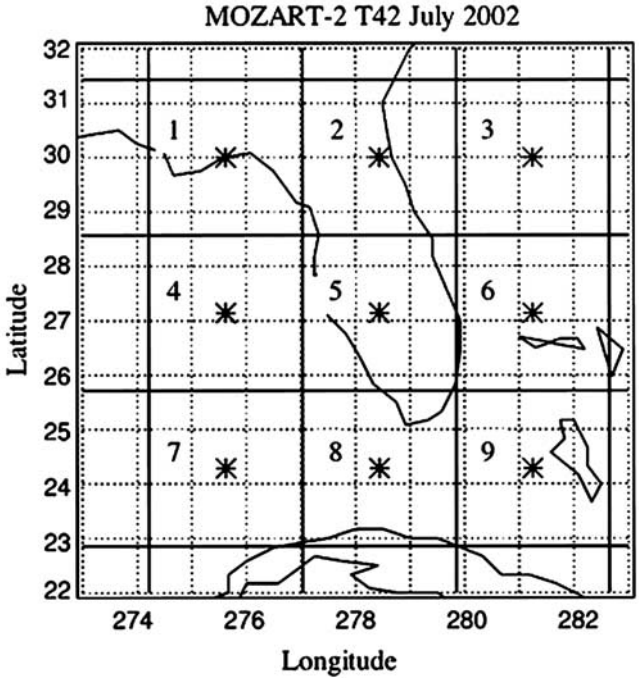

Figure 11. The nine grid points (indicated by stars) of the MOZART-2 CTM chosen for comparison with some of the observations made over the Florida area.

by Price et al. can be scaled to give any desired yearly global production rate (Tg(N)/yr). Here a global rate of 4 Tg(N)/yr was used but this choice has no bearing on the determination of the flash rates. The initial input of lightning-produced NO from both IC and CG flashes is scaled over the vertical extent (H) according to storm type as given by *Pickering et al.* [1998]. For example, for their midlatitude continental storm category the fraction by mass distributed above 5, 8, and 10 km would be 66%, 59%, and 47% if the storm height were 16 km. MOZART-2 scales these fractions over the actual calculated cloud top height. Thus both the initial vertical distribution and the flash rate depend on the cloud top height determined by the model convection.

[42] In the first comparison with the version of the model described by *Horowitz et al.* [2003], which was run here for July 2002 using the National Centers for Environmental Prediction (NCEP) input data, the model performed reasonably well for only the two continental cells 2 and 5: the NLDN(CG)/MOZART(CG) accumulated flash ratios for the month were ~2. Summing over all 9 cells of the Florida region the model underestimated just the CG flash accumulations by a factor of 4.6. For individual offshore cells the underestimate was much larger because the model assigned the F_{mar} flash rate expression solely on a geographic basis: the model formulation inadvertently missed the proposal by *Price and Rind* [1992] that a model cell be assigned as marine only if it was surrounded on four sides by other marine cells.

[43] When this revision was incorporated, the comparison of the results from the model with the CG flash accumulations derived the NLDN data is given in Table 5. For the true continental cells (1, 2, and 5), the model performs reasonably well: NLDN(CG)/MOZART(CG) accumulated flash ratios range from 1.9–2.4. Over the month, the model average cloud top height for these cells was 12.8 km whereas the aircraft or radar observations showed that cloud tops approached the tropopause height or were in the range of 14–15 km. Closer agreement would have been obtained had the model's convection achieved the altitude of the actual storms.

[44] For the cells located offshore (3, 4, 6, and 8), but now assigned the F_{cont} expression, the agreement on CG flash accumulations is quite good. MOZART overestimates the number of CG flashes in all but cell 6 by factors of only 1.3 to 1.5 and underestimates cell 6 by a factor of 0.83. That the NLDN derived CG accumulations are more often lower than the model is in agreement with results reported by *Molinié and Pontikis* [1995] that lightning flash rates in storms over the coast of French Guyana were intermediate to the F_{cont} and F_{mar} parameterizations.

[45] For the two cells (7, 9) of Table 5 classified as marine, the model results for CG accumulations remained much lower than observed. Clearly, the assignment of whether near-coastal cells, or those globally that contain larger islands, should use F_{mar} or F_{cont} is somewhat arbitrary and could be modified to achieve better agreement.

[46] The IC/CG ratios from the model over the month for the 9 cells range from 2.4–4.1 with an average of 3.4 ± 0.6, about 50% larger than the climatological ratio of 2–2.5 [*Boccippio et al.*, 2001]. If we use the climatological IC/CG ratio of 2.25 to estimate the total flash count from the NLDN data for the month, then the ratio of NLDN(IC + CG)/MOZART(IC + CG) = $3.25 \times 10^6/3.06 \times 10^6 = 1.1$, or there is remarkable agreement between the model results and those derived from the observations. Thus, although individual storms in July 2002 over Florida did not scale as $\sim H^{4.9}$, and although the model convection on average underestimated cloud top heights, compensations in the model parameterizations give a net result that is in reasonable accord with the observed flash accumulations and type for the month. On the other hand, if improvements in model convection or resolution lead to better agreement with observed cloud top heights, changes in the flash rate expressions would be required, especially for the coastal cells, to prevent significant overestimates of CG and IC flash accumulations.

[47] If we use the full range of P from Table 4 ($0.33–2.3 \times 10^{26}$ molecules NO/flash) simply as a scaling factor between the observations and the model, then the NLDN CG flash total (1.0×10^6 flashes) plus the climatological IC total (2.3×10^6 flashes) would yield a total mass of

Table 5. Flash Accumulations Over the Florida Region for July 2002

Cell	MOZART CG/1000	MOZART IC/1000	NLDN CG/1000
1 (C)[a]	95.9	357	178
2 (C)	88.3	353	167
3 (C)	90.5	334	60.2
4 (C)	88.3	359	52.1
5 (C)	93.3	356	227
6 (C)	91.3	299	110
7 (M)	0.51	1.75	38.2
8 (C)	97.8	354	74.0
9 (M)	0.54	1.54	93.7
Sum	647	2415	1000

[a]C, continental or considered continental; M, marine.

NO_x of 2.5–17.4 × 10^6 kg(N) for the 9 grid region of Figure 11. This run of MOZART-2 used P(CG) = 6 × 10^{26} molecules of NO/CG flash, 1/10th of that for IC flashes, and produced a mass of reactive nitrogen over the 9 grid region of 12 × 10^6 kg(N), near the midpoint of the range derived from the observations. Considering that the wide range from the observations is based on only two storms the model production is reasonably consistent.

6. Brief Comparison With Other Continental U.S. Storms

[48] Figure 12 gives a comparison of NO mixing ratios measured in two isolated storms over New Mexico [*Ridley et al.*, 1996], from a study of 11 storm complexes over the northeastern plains of Colorado [*Dye et al.*, 2000], and from the present study over Florida. We consider these composites as giving broad averages of the profile of NO in the anvils of thunderstorms for each area. As in Figures 1–3, most of the apparent spikes in NO are enhancements over many kilometers as the aircraft crossed through the anvils at constant altitude. The sampling in the anvil region in each project was similar, cross or longitudinal anvil passes and in the Colorado storms some spiral ascents or descents within the outflow. Thus we do not consider this gross comparison to be biased by the storm sampling protocol except that in the Florida project the WB-57F did not sample the underside of anvils nearer the core(s) below ~10 km, and in the Colorado project the Citation aircraft was not able to ascend to the highest regions of some anvils. In the New Mexico studies the Sabreliner aircraft was able to ascend above storm top on the August 12 flight. The mixing ratio range observed in the New Mexico and Colorado flights are also similar to nonsupercell studies made in Europe [*Huntrieser et al.*, 1998]. However, during the European Lightning Nitrogen Oxides project a supercell, dominated by IC activity, was investigated by multiple anvil transects over the more intense core region. Transects between 8 and 10 km found very large mixing ratios of NO from ~3–25 ppbv over distance scales of 0.3–2 km [*Huntrieser et al.*, 2002].

[49] The composite figures represent the net effects of LT/BL transport of NO_x and lightning production of NO to the UT for each continental region. Over New Mexico sampling in the LT/BL showed that the contribution to the NO_x observed in the anvil was minor (<10%) as would be expected for a reasonably remote continental region. Over Colorado, measurements of NO_x and other tracers with the NOAA P3 aircraft combined with model simulations [*DeCaria et al.*, 2000; *Skamarock et al.*, 2003] showed that the contribution from transport of NO_x from the LT/BL was

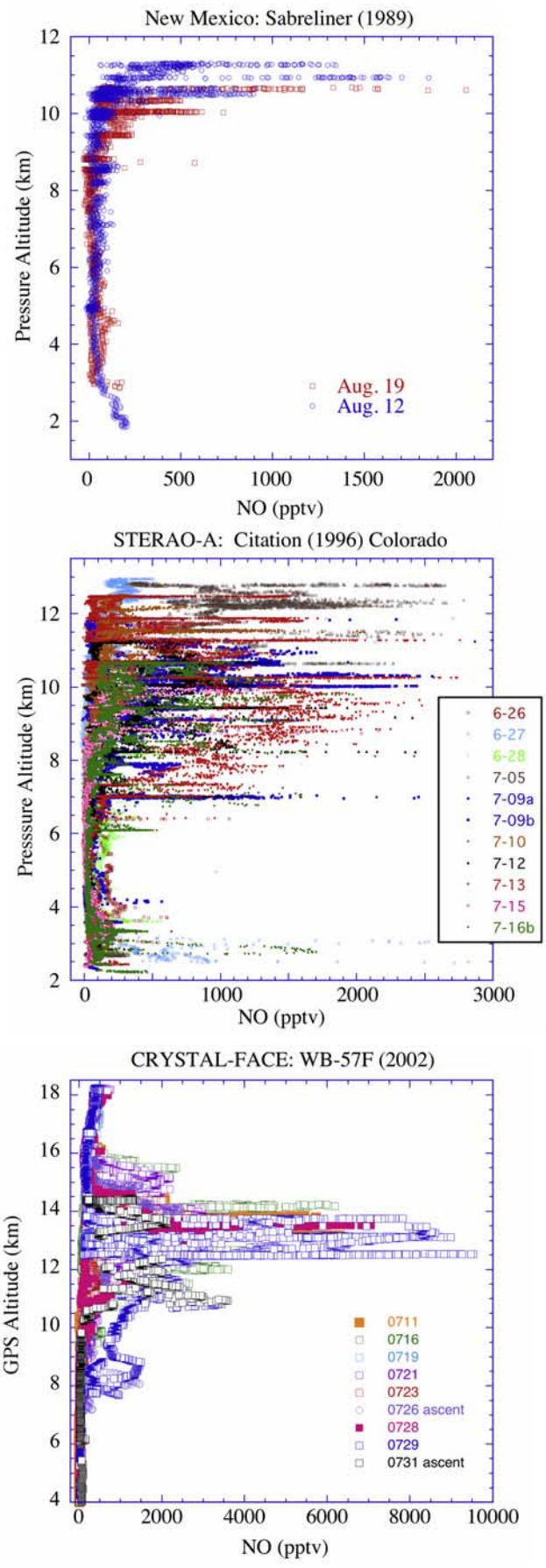

Figure 12. Vertical distributions of NO from thunderstorms over (top) New Mexico, (middle) Colorado plains, and (bottom) Florida. Note that the altitude and mixing ratio scales differ in each panel. A few small-scale spikes of NO larger than 3 ppbv in the Colorado storms are not shown [see *Stith et al.*, 1999]. Elevated NO below 4 km over New Mexico and Colorado was the result of pollution encountered on landing or takeoff near the respective airports. The New Mexico data are 2-s accumulations, and the others are 1-s accumulations.

in the range of 20–40%. In the absence of measurements of NO_x in the LT/BL in the Florida studies, we cannot define the contribution to the mixing ratios observed in the anvil passes.

[50] All three types of storms vent or produce high mixing ratios of reactive nitrogen to the UT, above about 7–10 km to anvil top, i.e., within the main anvil outflow region. The Colorado complexes cover a broader range (7–13 km) of outflow altitudes than the isolated storms studied over New Mexico and apparently a larger altitude range than observed over Florida, but this difference is due to the lack of sampling in the lower portions of the Florida anvils closer to the core(s). In all cases the venting can occur up to near the local tropopause, although largest mixing ratios of NO tend to be seen, especially in the Florida storms, 1–2 km below the tropopause.

[51] From these and the European studies it appears that a large fraction of the total lightning production and LT/BL transport of NO_x is vented to the UT but the aircraft observations made to date have not been able to quantify the fraction vented to say above 6–7 km for individual storms as discussed in the introduction. The altitude profile presentation for the New Mexico and Colorado studies in Figure 12 apparently supports the C-shaped distribution proposed by *Pickering et al.* [1998] where ~44% of the lightning-produced NO_x is distributed below 5 km for continental storms. However, the elevated NO (plus expected larger NO_2) measured below 4 km in the New Mexico and Colorado studies was due to pollution encountered on landing at the airports, not from measurements made near the bases of the storms. In the New Mexico study the aircraft investigated lower altitudes about the core and beneath one of the storms including an accidental transect of a hail shaft. In the Colorado study the NOAA P3 aircraft studied the low-altitude periphery of the storms but did not fly directly beneath the bases of the complexes [*Dye et al.*, 2000; *Skamarock et al.*, 2000]. Significantly elevated NO_x attributable to lightning was not found in either experiment near or below storm base but the chances of seeing results from individual CG flashes external to the core regions are small. Unlike the anvil region the output from flashes external to the core(s) is not integrated by storm dynamics. Enhanced NO_x comparable to the high mixing ratios of NO in the anvil was also not found in downdrafts but these regions are more difficult to find and examine compared to the anvil. The aircraft results do suggest that the downdraft region does not connect efficiently with the regions suffering lightning flashes. The low-altitude portion of the proposed C-shaped distribution was also absent in a model of a continental storm dominated by IC activity but where the downdraft was weak [*DeCaria et al.*, 2000]. *Skamarock et al.* [2003] found that their model downdraft originated at lower altitude than the origin of most flashes. Thus it is likely that the C-shaped distribution recommended for midlatitude continental storms discussed above overemphasizes the injection to the lower troposphere but more extensive and more difficult studies near the base of storms are required for quantification.

[52] The panels in Figure 12 display a significant trend in the range of maximum larger horizontal scale NO mixing ratios observed in the UT during thunderstorm activity over the three regions: New Mexico 1000–2000 pptv, Colorado 1500–3000 pptv, and Florida 2000–9500 pptv. However, the trend need not imply that typical Florida storms produce a larger mass of reactive nitrogen than typical Colorado storms. The latter storms can be longer-lived than those over Florida due to regeneration of convective cells as the storms translate over the more extensive plains. On the other hand, given the complexity of storm formation, of dynamics and mixing, ice/liquid particle formation, and of lightning physics and the temporal trends in all of these factors over the lifetime of a storm, it is perhaps surprising that the range of observed broad-scale maximum mixing ratios for reasonably electrically active continental storms is less than an order of magnitude.

7. Summary

[53] Although the CRYSTAL-FACE flights were not focused on examining the production of NO_x by thunderstorms, these observations made at near-tropical latitudes over Florida have reinforced earlier aircraft studies that showed that large amounts of NO_x were deposited to the upper troposphere from lightning production and from LT/BL transport. On portions of every flight, even in clear air, peak mixing ratios in the range of 1500–9500 pptv of NO were found illustrating that the chemistry of ozone production in the upper troposphere over the Florida region is strongly perturbed by thunderstorm activity, activity that remains high from June through August. In the Florida storms, injection occurred up to near the tropopause in some cases, but direct irreversible injection into the LS was minor compared to that into the UT. There were no examples of the convective systems strongly perturbing the local tropopause as has been reported for several midlatitude continental storms [*Poulida et al.*, 1996; *Stenchikov et al.*, 1996; *Dye et al.*, 2000].

[54] Observations from two isolated storm systems over Florida of quite different anvil size and electrical activity allowed approximate estimates of the total mass of NO_x vented to the middle and upper troposphere from lightning activity and LT/BL transport. Using the CG flash accumulations derived from the NLDN data, climatological IC/CG ratios, and assuming that CG and IC flashes were of equivalent efficiency for NO production, the ranges of production per average flash for the moderate-sized (0716) and the large storm (0729) were significantly different at $(0.33–0.66) \times 10^{26}$ and $(1.7–2.3) \times 10^{26}$ molecules/flash, respectively. Based on the average global flash rate of 44 s^{-1} [*Christian et al.*, 2003], these two storms yield global annual production rates of 1.1–2.2 and 5.5–7.5 Tg(N)/yr, respectively. Making the more usual assumption that IC efficiency is 1/10th that of CG activity, the ranges of production per CG flash for the moderate-sized and large storm were $(0.88–1.8) \times 10^{26}$ and $(4.5–6.1) \times 10^{26}$, respectively. The estimates from the 0716 storm are considered to be less uncertain than those from the 0729 storm because there was indirect evidence that the latter sustained significantly more IC activity than climatology would suggest. The estimated ranges of production per average flash or per CG flash could be high due to the unknown magnitude of the contribution from transport of reactive nitrogen from the LT/BL.

[55] In contrast to some climatological analyses, the lightning flash rates for these two storms did not scale as $\sim H^5$. Indeed, all of the storms studied with the WB-57F over the month of July reached a fairly narrow range of maximum cloud top altitudes (14–15 km), yet quite different flash rates occurred.

[56] The observed CG flash accumulations and NO_x mass production estimate for the month of July 2002 over the Florida area were compared with the MOZART-2 CTM using T42 resolution, NCEP input data, and the *Price and Rind* [1992, 1994] and *Price et al.* [1997a] lightning flash parameterizations. When the original model formulation was corrected to include the assignment of continental versus marine flash rate expressions recommended by *Price and Rind* [1992], the model flash type and accumulations were in good agreement with those derived from the NLDN data. Some compensation occurred between the model underestimate of CG flashes in grid cells over land and the overestimate in most grid cells located offshore. The model underestimated actual cloud top heights by 1–2 km, a result that has at least two important consequences. First the flash rate parameterization of *Price and Rind* [1992] is quite sensitive to cloud top height and thus is the mass of lightning-produced NO. Second, the lifetime of NO_x is strongly dependent on altitude: correct injection to the UT is more important chemically than injection to the middle and lower troposphere where the lifetime is much shorter. Indeed it is more important chemically to refine the global budget of NO_x production by lightning for altitudes above about 6 km than it is to refine the total over all altitudes.

[57] A comparison of continental storms over the United States revealed that broad-scale (20–175 km) median mixing ratios of NO within the anvil outflow were larger in the order Florida (2000–9500 pptv) > Colorado (1500–3000 pptv) > New Mexico (1000–2000 pptv). This result does not mean that Florida storm complexes produce a larger mass of reactive nitrogen as some central plains storms have electrically active lifetimes considerably longer than those over Florida.

[58] **Acknowledgments.** We thank the pilots and crew of the NASA WB-57F for providing the flights, the Upper Atmospheric Research Program (M. Kurylo) and the Radiation Science Program of NASA (D. Anderson) for providing support, and L. Nguyen of the NASA Langley Research Center for providing the GOES and flight track images. The NLDN data were collected by Vaisala-Thunderstorm and supplied to us by the Global Hydrology Resource Center at NASA Marshall Space Flight Center. MTP measurements were made under contract from NASA to the Jet Propulsion Laboratory, California Institute of Technology. NCAR is operated by the University Corporation for Atmospheric Research under sponsorship of the National Science Foundation.

References

Allen, D. J., and K. E. Pickering (2002), Evaluation of lightning flash rate parameterizations for use in a global chemical transport model, *J. Geophys. Res.*, *107*(D23), 4711, doi:10.1029/2002JD002066.

Baumgardner, D., H. Jonsson, W. Dawson, D. O'Conner, and R. Newton (2002), The Cloud, Aerosol and Precipitation Spectrometer (CAPS): A new instrument for cloud investigations, *Atmos. Res.*, *59–60*, 252–264.

Boccippio, D. J., K. L. Cummins, H. J. Christian, and S. J. Goodman (2001), Combined satellite- and surface-based estimation of the intracloud to cloud-to-ground lightning ratio over the continental United States, *Mon. Weather Rev.*, *129*, 108–129.

Brasseur, G. P., D. A. Hauglustaine, S. Walters, P. J. Rasch, J.-F. Müller, C. Granier, and X. X. Tie (1998a), MOZART, a global chemical transport model for ozone and related chemical tracers: 1. Model description, *J. Geophys. Res.*, *103*, 28,265–28,289.

Brasseur, G. P., R. A. Cox, D. Hauglustaine, I. Isaksen, J. Lelieveld, D. H. Lister, R. Sausen, U. Schumann, A. Wahner, and P. Wiesen (1998b), European scientific assessment of the atmospheric effects of aircraft emissions, *Atmos. Environ.*, *32*, 2329–2418.

Brooks, C. E. P. (1925), The distribution of thunderstorms over the globe, *Meteorol. Off. Geophys. Memo., Dubl.*, *3*, 147–164.

Brunner, D., J. Staehelin, D. Jeker, H. Wernli, and U. Schumann (2001), Nitrogen oxides and ozone in the tropopause region of the Northern Hemisphere: Measurements from commercial aircraft in 1995/1996 and 1997, *J. Geophys. Res.*, *106*, 27,673–27,699.

Christian, H. J., et al. (2003), Global frequency and distribution of lightning as observed from space by the Optical Transient Detector, *J. Geophys. Res.*, *108*(D1), 4005, doi:10.1029/2002JD002347.

Crawford, J., et al. (2000), Evolution and chemical consequences of lightning-produced NO_x observed in the North Atlantic upper troposphere, *J. Geophys. Res.*, *105*, 19,795–19,809.

Cummins, K. L., M. J. Murphy, E. A. Bardo, W. L. Hiscox, R. B. Pyle, and A. E. Pifer (1998), A combined TOA/MDF technology upgrade of the U.S. National Lightning Detection Network, *J. Geophys. Res.*, *103*, 9035–9044.

DeCaria, A. J., K. E. Pickering, G. L. Stenchikov, J. R. Scala, J. L. Stith, J. E. Dye, B. A. Ridley, and P. Laroche (2000), A cloud-scale model study of lightning-generated NO_x in an individual thunderstorm during STERAO-A, *J. Geophys. Res.*, *105*, 11,601–11,616.

Defer, E., P. Blanchet, C. Théry, P. Laroche, J. E. Dye, M. Venticinque, and K. L. Cummins (2001), Lightning activity for the July 10, 1996, storm during the Stratosphere-Troposphere Experiment: Radiation, Aerosol. and Ozone-A (STERAO-A) experiment, *J. Geophys. Res.*, *106*, 10,151–10,172.

Dickerson, R. R., et al. (1987), Thunderstorms: An important mechanism in the transport of pollutants, *Science*, *235*, 460–465.

Dye, J. E., et al. (2000), An overview of the Stratospheric-Tropospheric Experiment: Radiation, Aerosols, and Ozone (STERAO)-Deep Convection experiment with results for the July 10, 1996, storm, *J. Geophys. Res.*, *105*, 10,023–10,045.

Ehhalt, D. H., and F. Rohrer (1995), The impact of commercial aircraft on tropospheric ozone, in *The Chemistry of the Atmosphere-Oxidants and Oxidation in the Earth's Atmosphere*, *Spec. Publ. 170*, edited by A. R. Bandy, pp. 105–120, R. Soc. of Chem., Cambridge, UK.

Ehhalt, D. H., F. Rohrer, and A. Wahner (1992), Sources and distribution of NO_x in the upper troposphere at northern midlatitudes, *J. Geophys. Res.*, *97*, 3725–3738.

Fehr, T., H. Höller, and H. Huntrieser (2004), Model study on production and transport of lightning-produced NO_x in a EULINOX supercell storm, *J. Geophys. Res.*, *109*, D09102, doi:10.1029/2003JD003935.

Flatøy, F., and Ø. Hov (1997), NO_x from lightning and the calculated chemical composition of the free troposphere, *J. Geophys. Res.*, *102*, 21,373–21,381.

Gallardo, L., and V. Cooray (1996), Could cloud-to-cloud discharges be as effective as cloud-to-ground discharges in producing NO_x?, *Tellus, Ser. B*, *48*, 641–651.

Heymsfield, G. M., S. Bidwell, I. J. Caylor, S. Ameen, S. Nicholson, W. Boncyk, L. Miller, D. Vandemark, P. E. Racette, and L. R. Dod (1996), The EDOP radar system on the high altitude NASA-ER-2 aircraft, *J. Atmos. Oceanic Technol.*, *13*, 795–809.

Horowitz, L. W., et al. (2003), A global simulation of tropospheric ozone and related tracers: Description and evaluation of MOZART, version 2, *J. Geophys. Res.*, *108*(D24), 4784, doi:10.1029/2002JD002853.

Huntrieser, H., H. Schlager, C. Feigl, and H. Höller (1998), Transport and production of NO_x in electrified thunderstorms: Survey of previous studies and new observations at midlatitudes, *J. Geophys. Res.*, *103*, 28,247–28,264.

Huntrieser, H., et al. (2002), Airborne measurements of NO_x, tracer species, and small particles during the European Lightning Nitrogen Oxides Experiment, *J. Geophys. Res.*, *107*(D11), 4113, doi:10.1029/2000JD000209.

Intergovernmental Panel on Climate Change (IPCC) (2001), *Climate Change 2001: The Scientific Basis—Contribution of Working Group I to the Third Assessment Report of the Intergovernmental Panel on Climate Change*, edited by J. T. Houghton et al., p. 260, Cambridge Univ. Press, New York.

Jaeglé, L., et al. (2000), Photochemistry of HO_x in the upper troposphere at northern latitudes, *J. Geophys. Res.*, *105*, 3877–3892.

Jeker, D. P., L. Pfister, A. M. Thompson, D. Brunner, D. J. Boccippio, K. E. Pickering, H. Wernli, Y. Kondo, and J. Staehelin (2000), Measurements of nitrogen oxides at the tropopause: Attribution to convection and correlation with lightning, *J. Geophys. Res.*, *105*, 3679–3700.

Jensen, E., O. B. Toon, D. L. Westphal, S. Kinne, and A. J. Heymsfield (1994), Microphysical modeling of cirrus: 1. Comparison with 1986 FIRE IFO measurements, *J. Geophys. Res.*, *99*, 10,421–10,442.

Jensen, E., D. Starr, and O. Toon (2004), Mission investigates tropical cirrus clouds, *Eos Trans. AGU*, *85*(5), 45.

Lamarque, J.-F., G. P. Brasseur, P. G. Hess, and J.-F. Müller (1996), Three-dimensional study of the relative contributions of the different nitrogen sources in the troposphere, *J. Geophys. Res.*, *101*, 22,955–22,968.

Lange, L., et al. (2001), Detection of lightning-produced NO in the mid-latitude upper troposphere during STREAM 1998, *J. Geophys. Res.*, *106*, 27,777–27,785.

Langford, A. O., R. W. Portmann, J. S. Daniel, H. L. Miller, and S. Solomon (2004), Spectroscopic measurements of NO_2 in a Colorado thunderstorm: Determination of the mean production by cloud-to-ground lightning flashes, *J. Geophys. Res.*, *109*, D11304, doi:10.1029/2003JD004158.

Lawrence, M. G., W. L. Chameides, P. S. Kasibhatla, H. Levy II, and W. Moxim (1995), Lightning and atmospheric chemistry: The rate of atmospheric NO production, in *Handbook of Atmospheric Electrodynamics*, vol. 1, edited by H. Volland, pp. 189–202, CRC Press, Boca Raton, Fla.

Levy, H., II, W. J. Moxim, and P. S. Kasibhatla (1996), A global three-dimensional time-dependent lightning source of tropospheric NO_x, *J. Geophys. Res.*, *101*, 22,911–22,922.

Li, L., G. M. Heymsfield, P. E. Racette, L. Tian, and E. Zenker (2004), A 94 GHz cloud radar system on a NASA high-altitude ER-2 aircraft, *J. Atmos. Oceanic Technol.*, in press.

Madronich, S. (1987), Photodissociation in the atmosphere: 1. Actinic flux and the effects of ground reflections and clouds, *J. Geophys. Res.*, *92*, 9740–9752.

McGill, M. J., D. L. Hlavka, W. D. Hart, V. S. Scott, J. D. Spinhirne, and B. Schmid (2002), The Cloud Physics Lidar: Instrument description and initial measurement results, *Appl. Opt.*, *41*, 3725–3734.

Meijer, E. W., P. F. J. van Velthoven, A. M. Thompson, L. Pfister, H. Schlager, P. Schulte, and H. Kelder (2000), Model calculations of the impact of NO_x from air traffic, lightning, and surface emissions, compared with measurements, *J. Geophys. Res.*, *105*, 3833–3850.

Molinié, J., and C. A. Pontikis (1995), A climatological study of tropical thunderstorm clouds and lightning frequencies on the French Guyana coast, *Geophys. Res. Lett.*, *22*, 1085–1088.

Nesbitt, S. W., R. Zhang, and R. E. Orville (2000), Seasonal and global NO_x production by lightning estimated from the optical transient detector (OTD), *Tellus, Ser. B*, *52*, 1206–1215.

Pickering, K. E., A. M. Thompson, J. R. Scala, W.-K. Tao, R. R. Dickerson, and J. Simpson (1992), Free tropospheric ozone production following entrainment of urban plumes into deep convection, *J. Geophys. Res.*, *97*, 17,985–18,000.

Pickering, K. E., et al. (1996), Convective transport of biomass burning emissions over Brazil during TRACE-A, *J. Geophys. Res.*, *101*, 23,993–24,012.

Pickering, K. E., Y. Wang, W.-K. Tao, C. Price, and J.-F. Müller (1998), Vertical distributions of lightning NO_x for use in regional and global transport models, *J. Geophys. Res.*, *103*, 31,203–31,216.

Poulida, O., R. R. Dickerson, and A. Heymsfield (1996), Stratospheric-troposphere exchange in a midlatitude mesoscale convective complex: 1. Observations, *J. Geophys. Res.*, *101*, 6823–6836.

Price, C., and D. Rind (1992), A simple lightning parameterization for calculating global lightning distributions, *J. Geophys. Res.*, *97*, 9919–9933.

Price, C., and D. Rind (1994), Modeling global lightning distributions in a general circulation model, *Mon. Weather Rev.*, *122*, 1930–1939.

Price, C., J. Penner, and M. Prather (1997a), NO_x from lightning: 1. Global distribution based on lightning physics, *J. Geophys. Res.*, *102*, 5929–5941.

Price, C., J. Penner, and M. Prather (1997b), NO_x from lightning: 2. Constraints from the global atmospheric electric circuit, *J. Geophys. Res.*, *102*, 5943–5951.

Ridley, B. A., J. E. Dye, J. G. Walega, J. Zheng, F. E. Grahek, and W. Rison (1996), On the production of active nitrogen by thunderstorms over New Mexico, *J. Geophys. Res.*, *101*, 20,985–21,005.

Ridley, B., et al. (2004), Convective transport of reactive constituents to the tropical and midlatitude tropopause region: I. Observations, *Atmos. Environ.*, *38*, 1259–1274.

Siewert, J., K. Davison, W. Frank, and J. Verlinde (2003), CRYSTAL-FACE convective drafts, *Eos Trans. AGU*, *84*(46), Fall Meet. Suppl., Abstract A11B-04.

Skamarock, W. C., J. G. Powers, M. Barth, J. E. Dye, T. Matejka, D. Bartels, K. Baumann, J. Stith, D. D. Parrish, and G. Hübler (2000), Numerical simulations of the 10 July STERAO/Deep Convection experiment convective system: Kinematics and transport, *J. Geophys. Res.*, *105*, 19,973–19,990.

Skamarock, W. C., J. E. Dye, E. Defer, M. C. Barth, J. L. Stith, and B. A. Ridley (2003), Observations- and modeling-based budget of lightning-produced NO_x in a continental thunderstorm, *J. Geophys. Res.*, *108*(D10), 4305, doi:10.1029/2002JD002163.

Stenchikov, G., R. Dickerson, K. Pickering, W. Ellis Jr., B. Doddridge, S. Kondragunta, O. Poulida, J. Scala, and W.-K. Tao (1996), Stratosphere-troposphere exchange in a midlatitude mesoscale convective complex: 2. Numerical simulations, *J. Geophys. Res.*, *101*, 6837–6851.

Stith, J., J. Dye, B. Ridley, P. Laroche, E. Defer, K. Baumann, G. Hübler, R. Zerr, and M. Venticinque (1999), NO signatures from lightning flashes, *J. Geophys. Res.*, *104*, 16,081–16,089.

Théry, C., P. Laroche, and P. Blanchet (2000), Lightning activity during EULINOX and estimations of NO_x production by flashes, in *EULINOX—The European Lightning Nitrogen Oxides Experiment*, *DLR Forschungsber. 2000-28*, pp. 129–145, Deutsches Zentrum für Luft- und Raumfahrt, Cologne, Germany.

Tie, X. X., R. Zhang, G. Brasseur, and W. Lei (2002), Global NO_x production by lightning, *J. Atmos. Chem.*, *43*, 61–74.

Ushio, T., S. J. Heckman, D. J. Boccippio, H. J. Christian, and Z.-I. Kawasaki (2001), A survey of thunderstorm flash rates compared to cloud top height using TRMM satellite data, *J. Geophys. Res.*, *106*, 24,089–24,095.

World Meteorological Organization (WMO) (1995), Scientific assessment of ozone depletion: 1994, *Rep. 37*, Global Ozone Res. and Monit. Proj., Geneva.

Zhang, R., X. Tie, and D. W. Bond (2003), Impacts of anthropogenic and natural NO_x sources over the U.S. on troposphere chemistry, *Proc. Natl. Acad. Sci. U. S. A.*, *100*, 1505–1509.

Zhang, X., J. H. Helsdon Jr., and R. D. Farley (2003a), Numerical modeling of lightning-produced NO_x using an explicit lightning scheme: 1. Two-dimensional simulations as a "proof of concept," *J. Geophys. Res.*, *108*(D18), 4579, doi:10.1029/2002JD003224.

Zhang, X., J. H. Helsdon Jr., and R. D. Farley (2003b), Numerical modeling of lightning-produced NO_x using an explicit lightning scheme: 2. Three-dimensional simulation and expanded chemistry, *J. Geophys. Res.*, *108*(D18), 4580, doi:10.1029/2002JD003225.

D. Baumgardner, Centro de Ciencias de la Atmosfera, Universidad Nacional Autonoma de Mexico, Circuito Exterior, Ciudad Universitaria, 04510 Mexico D. F., Mexico. (darrel@servidor.unam.mx)

G. Brasseur and M. Schultz, Max Planck Institute für Meteorologie, Bundesstrasse 55, 20146 Hamburg, Germany. (brasseur@dkrz.de; martin.schultz@dkrz.de)

L. Emmons, F. Grahek, D. Knapp, D. Montzka, B. Ridley, and A. Weinheimer, Atmospheric Chemistry Division, National Center for Atmospheric Research, P.O. Box 3000, Boulder, CO 80307-3000, USA. (emmons@ucar.edu; knarf@ucar.edu; dave@ucar.edu; montzka@ucar.edu; ridley@ucar.edu; wein@ucar.edu)

G. Heymsfield and M. McGill, Mesoscale Atmospheric Processes Branch, Code 912, NASA Goddard Space Flight Center, Greenbelt, MD 20771, USA. (heymsfield@agnes.gsfc.nasa.gov; mcgill@agnes.gsfc.nasa.gov)

P. Kucera, Department of Atmospheric Sciences, University of North Dakota, P.O. Box 9006, Grand Forks, ND 58202, USA. (pkucera@aero.und.edu)

L. Li, Goddard Earth Sciences and Technology Center, University of Maryland, 1000 Hilltop Circle, Baltimore, MD 21250, USA. (lihua@agnes.gsfc.nasa.gov)

M. J. Mahoney, Jet Propulsion Laboratory, California Institute of Technology, Mail Stop 246-102, NASA, 4800 Oak Grove Drive, Pasadena, CA 91109-8099, USA. (michael.j.mahoney@jpl.nasa.gov)

L. Ott and K. Pickering, Department of Meteorology, University of Maryland, College Park, MD 20742, USA. (leo@atmos.umd.edu; pickerin@atmos.umd.edu)